Carbon budgets of Scotia Sea mesopelagic zooplankton and micronekton communities during austral spring

Authors: Kathryn B. Cook[1,6*], Anna Belcher[2], Daniel Bondyale Juez[3], Gabriele Stowasser[2], Sophie Fielding[2], Ryan A. Saunders[2], Mohamed A. Elsafi[4], George A. Wolff[5], Sabena J. Blackbird[5], Geraint A. Tarling[2], Daniel J. Mayor[1,6]

[1] National Oceanography Centre, Southampton, SO14 3ZH, UK

[2] British Antarctic Survey, Cambridge, CB3 0ET, UK

[3] EOMAR, Universidad de Las Palmas de Gran Canaria, Spain

[4]Oceanography Department, Faculty of Science, Alexandria University, Egypt

[5]School of Environmental Sciences, University of Liverpool, Liverpool, L69 3GP, UK

[6]Department of Biosciences, University of Exeter, Exeter, EX4 4PS

*Corresponding author: k.cook@exeter.ac.uk, +44 (0)1392 726306

Abstract

Zooplankton form an integral component of epi- and mesopelagic ecosystems, and there is a need to better understand their role in ocean biogeochemistry. The export and remineralisation of particulate organic matter at depth plays an important role in controlling atmospheric CO_2 concentrations. Pelagic mesozooplankton and micronekton communities may influence the fate of organic matter in a number of ways, including: the consumption of primary producers and export of this material as fast-sinking faecal pellets, and the active flux of carbon by animals undertaking diel vertical migration (DVM) into the mesopelagic. We present day and night vertical biomass profiles of mesozooplankton and micronekton communities in the upper 500 m during three visits to an ocean observatory station (P3) to the NW of South Georgia (Scotia Sea, South Atlantic) in austral spring, alongside estimates of their daily rates of ingestion and respiration throughout the water column. Day and night community biomass estimates were dominated by copepods >330 µm, including the lipid-rich species, *Calanoides acutus* and *Rhincalanus gigas*. We found little evidence of synchronised DVM, with only *Metridia* spp. and *Salpa thompsoni* showing patterns consistent with migratory behaviour. At depths below 250 m, estimated community carbon ingestion rates exceeded those of metabolic costs, supporting the understanding that food quality in the

mesopelagic is relatively poor, and organisms have to consume a large amount of food in order to fulfil their nutritional requirements. By contrast, estimated community rates of ingestion and metabolic costs at shallower depths were approximately balanced, but only when we assumed that the animals were predominantly catabolising lipids (i.e. respiratory quotient = 0.7) and had relatively high absorption efficiencies. Our work demonstrates that it is possible to balance the metabolic budgets of mesopelagic animals to within observational uncertainties, but highlights the need for a better understanding of the physiology of lipid-storing animals and how it influences carbon budgeting in the pelagic.

Keywords:

Biological Gravitational Pump; Zooplankton; Micronekton; Respiration; Ingestion; Carbon; Scotia Sea; Lipids

1 Introduction

The photosynthetic production of organic matter in the surface ocean, and its subsequent export and remineralisation at depth, plays a fundamental role in controlling atmospheric CO_2 levels (Boyd et al., 2019). The depth at which sinking organic particles are consumed and respired by midwater organisms influences the timeframe over which the constituent carbon is isolated from the atmosphere and hence 'sequestered' (Kwon et al., 2009). Quantifying and understanding the myriad processes that make up the ocean's 'biological gravitational pump' (BGP), and how it will respond to future climate, remain major goals of contemporary biological oceanography.

The majority of sinking particulate organic matter (POM) that leaves the base of the euphotic zone is remineralised within the mesopelagic zone, which extends down to 1,000 m (Buesseler et al., 2007; Steinberg et al., 2008; Giering et al., 2014). The collective respiratory demands of organisms within this zone should, at steady state, equal the removal of sinking carbon flux. However, until recently, attempts to compare the biological requirements for organic carbon with that supplied have produced considerable mismatches, with the former exceeding the latter by up to two orders of magnitude (reviewed by Burd et al., 2010). In 2014, the first balanced mesopelagic carbon budget was published for the long-term monitoring site at the Porcupine Abyssal Plain, NE Atlantic (Giering et al., 2014), highlighting the importance of mesopelagic animals and their interactions with sinking particles. Zooplankton and micronekton communities contribute to, and interact with, the BGP passively *via* the production of sinking particles such as faecal pellets and carcasses, and actively *via* feeding on sinking particles and through diel vertical migrations (DVM) which remove carbon from surface waters and transport it to below the euphotic zone (See reviews by Steinberg and Landry, 2017; Le Moigne, 2019).

Zooplankton and micronekton feeding in the epipelagic re-package slow-sinking organic matter into dense, faster sinking faecal pellets that increase the gravitational flux of carbon (Turner, 2015). The magnitude of particle flux and sinking speeds varies with pelagic community biomass, composition, grazing rates and behaviour (Zøllner et al., 2009; Manno et al., 2015; Belcher et al., 2016; Polimene et al., 2017; Belcher et al., 2019a; Liszka et al., 2019; Yang et al., 2019). Particle sinking speeds, including those of faecal pellets, can be modified through fragmentation (Briggs et al., 2020). Indeed, particle fragmentation by the feeding activities of zooplankton resident in the mesopelagic has been suggested to arrest a significant fraction of the sinking flux and may therefore influence how deep particles penetrate into the ocean's interior (Mayor et al., 2014; Mayor et al., 2020).

DVM of zooplankton and micronekton, where animals reside at depth during the day and migrate to feed at the surface at night, is widely reported in marine ecosystems (reviewed by Bandara et al.,

2021). These migrations actively transport carbon ingested in the epipelagic to the mesopelagic where it may be released via excretion, respiration, egestion and mortality at depth (Steinberg and Landry, 2017 and references therein), and so are often incorporated into biogeochemical models (e.g. Longhurst et al., 1990; Hansen and Visser, 2016; Archibald et al., 2019; Kelly et al., 2019). Mesopelagic micronekton can generate a significant proportion of total respiratory fluxes (e.g. Hidaka et al., 2001; Ariza et al., 2015; Belcher et al., 2019b), but direct measurements from the mesopelagic are limited as it is difficult to collect animals for incubation measurements without damaging them, and it is also hard to replicate the changing temperature and pressure conditions experienced *in situ* during migration. Mesopelagic organisms can therefore play an important role in the biological carbon pump, yet quantifying how they affect the numerous carbon flow pathways that they are involved in remains challenging.

The COMICS (Controls over Ocean Mesopelagic Interior Carbon Storage) programme was designed to deliver new insights into the processes influencing carbon cycling in the mesopelagic zone and hence the storage of carbon in the ocean (Sanders et al., 2016). Quantifying the vertical distribution and movements of zooplankton, along with their feeding behaviours and metabolic requirements, is integral to understanding how ocean biology contributes to this process. The region downstream from South Georgia in the Scotia Sea, South Atlantic, is an iron-fertilised hotspot of productivity that supports an extensive phytoplankton bloom and high biomass of mesozooplankton and micronekton (Korb et al., 2012; Ward et al., 2012), resulting in high levels of carbon export to the deep ocean. Station P3, a long-term mooring observatory (Scotia Sea open-ocean biological programme of Sustained Observation, British Antarctic Survey, NERC; Manno et al., 2015) in this region, which forms part of a programme of sustained observations in the open-ocean Scotia Sea, was chosen as the site for COMICS fieldwork (Sanders et al., 2016). Day and night depth profiles of mesozooplankton and micronekton biomass were collected to estimate the magnitude of DVM. The respiration rates of mesozooplankton and micronekton communities were determined using a combination of Electron Transport System (ETS) and biomass measurements combined with allometric calculations. Grazing experiments were also conducted for resident and potentially migratory mesopelagic mesozooplankton species. These data were used to generate carbon budgets of the mesopelagic zooplankton and micronekton communities in the Scotia Sea.

2 Methods

Sampling for this study was conducted during a research cruise to the Scotia Sea in the Southern Ocean in austral spring (DY086; 12 November 2017 – 19 December 2017) aboard the *RRS Discovery*

(cruise report: Giering et al., 2019a). Sampling was focused at station P3, a long-term observation site (Tarling et al., 2012; Manno et al., 2015; Manno et al., 2022), located to the northwest of South Georgia (52.40 °S, 40.06°W). The same station was occupied on three occasions, defined as stations P3A (15 - 22nd November), P3B (29th November – 5th December) and P3C (9 – 15th December). Vertical profiles of temperature were obtained from Conductivity-Temperature-Depth (CTD) unit (SBE 9 plus) deployments. Daylight hours and lunar phase for each sampling date were taken from SunriseSunset.com for the latitude and longitude of P3.

2.1 Mesozooplankton and micronekton

2.1.1 Net sampling

To effectively sample across the size range of organisms (0.1mm – 300 mm) encompassed by the classifications of mesozooplankton to micronekton, we required a multi-net-sampling strategy (Table 1) as a result of differing sampling efficiencies (Wiebe and Benfield, 2003). A Hydrobios Mammoth Net (hauled at 0.2 ms^{-1}) and a motion-compensated opening/closing Bongo net (hauled at 0.3 ms^{-1}) were deployed vertically to sample mesozooplankton. The Bongo was generally set out in two sequential deployments with one sampling the top 150 m, and the other sampling from 150m to 500 m. Mammoth deployments were repeated day and night, but Bongo deployments for biomass measurements only took place during the day. Additional Bongo deployments at the same depths were made in order to collect live animals for grazing experiments. The water volumes filtered by the Bongo and Mammoth nets were calculated using the net dimensions and depth of water sampled assuming 100% efficiency (Ward et al., 2012).

To collect the larger mesozooplankton and micronekton, we deployed a MOCNESS (Multiple Opening and Closing Nets and Environmental Sampling System, Wiebe and Benfield, 2003) and an RMT25 (opening and closing 25 m^2 rectangular mid-water trawl net, Baker et al., 1973; Piatkowski et al., 1994). Both nets were towed obliquely at a speed of 2 knots, and deployments were repeated day and night. The MOCNESS was towed for 10 minutes in each depth layer, and the volume filtered was calculated using a flow meter and estimated effective mouth area. The RMT was towed for 40 minutes in each depth layer, and the volume filtered was calculated using the net dimensions and the distance travelled by the net.

Table 1: Summary of multi-net sampling strategy. Bongo nets were only deployed during the day, all other net deployments were repeated day and night.

Sampler	Target group	Mesh size (mm)	Mouth area (m^2)	Net depth strata (m)	Analysis
Bongo (n = 16)	Small mesozooplankton: microcopepods, small calanoid copepods	0.1	0.29	0-150 150-500	- Abundance FlowCam Macro - Biomass Abundance × mass (Table S2) - Community respiration Whole sample ETS - Copepod grazing (Table 2) - Community ingestion Biomass × daily ration (Table S7)
Bongo (n = 1)	Small mesozooplankton: microcopepods, small calanoid copepods	0.1	0.29	0-75 75-150 150-250 250-500	- Biomass specific respiration Whole sample ETS
Mammoth (n = 4)	Mesozooplankton: large calanoid copepods, larval euphausiids	0.3	1	0-33 33-63 63-125 125-188 188-250 250-313 313-375 375-438 438-500	- Biomass specific respiration Whole sample ETS
MOCNESS (n = 4)	Large mesozooplankton and small micronekton: fast swimming small euphausiids, chaetognaths, salps	0.33	1	0-62 62-125 125-187 187-250 250-312 312-375 375-437 437-500	- Abundance Manual - Biomass Abundance × mass (Ward et al., 2012) - Community respiration Biomass × specific respiration - Community ingestion Biomass × daily ration (Table S7)
RMT25 (n = 6)	Micronekton: Krill, mesopelagic fish, cephalopods, large cnidarians	4	25	0-250 250-500	- Wet weight (WW) - Biomass WW:Dry Mass (DM; Tables S5, S6) -Community respiration Individual ETS (Fish, euphausiids) WW to respiration (Tables S3) DM to respiration (Table S4) - Community ingestion Biomass × daily ration (Table S7)

142

2.2 Sample handling and biomass measurements

2.2.1 Biomass

One net of the Bongo catches was preserved in 4% borax buffered formaldehyde for particle enumeration using a FlowCam Macro (Yokogawa Fluid Imaging Technologies Inc.). One set of preserved Bongo samples was also sent to the NMFRI Plankton Sorting and Identification Centre, Poland, for species identification and enumeration.

MOCNESS catches were split into two aliquots, using a Folsom plankton splitter, with one half being preserved in 4% borax buffered formaldehyde for biomass analysis. These were sent to the NMFRI Plankton Sorting and Identification Centre, Poland, for species identification and enumeration of subsamples containing at least 500 individuals, and the data were used to calculate biomass by applying a published mass factor to each taxonomic entity (Ward et al., 2012). For euphausiids sampled by the MOCNESS net (all except *Euphausia superba* where composite weight was measured from the RMT25) we estimated the biomass of the enumerated species using literature-derived estimates of wet mass (WM). For *Thysanoessa* spp. we estimated a representative WM of 46.6 mg using a length of 20 mm taken from Siegel (1987) and the length-weight relationship of Siegel (1992). For the remaining euphausiid species (of which *Euphausia frigida* was the dominant species), we estimated a representative WM of 34.5 mg using a mean length of 18 mm (Kittel et al., 1985; Siegel, 1987) and the relationship of Siegel (1992). The second MOCNESS aliquot was used to collect animals for other analyses including lipid content. Replicate samples of two C6 female *Rhincalanus gigas* or five C5 *Calanoides acutus* were rapidly picked into glass vials in a controlled temperature laboratory set at the *in situ* surface temperature (2 °C) and immediately stored at -80 °C.

RMT25 catches were analysed immediately to determine taxonomic composition, abundance and WM of the whole sample. Fish were identified and weighed individually, whilst other taxa were counted and weighed in batches. The mean individual WM of micronekton species from the RMT25 net was calculated using the total abundance and total WM for each species.

Weighted Mean Depth (WMD) of total biomass and selected taxa from the MOCNESS and RMT nets were calculated using equation 1:

$$\text{WMD (m)} = \sum(b_i \times d_i) / B \qquad \text{(eq 1)}$$

Where b_i is the biomass (mg C m^{-3}) in net *i*, d_i is the mid-depth (m) of net *i*, and B is the biomass in all nets. Day WMD was subtracted from night WMD to determine the depth change due to diel migration (ΔWMD).

2.2.2 FlowCam Macro

The preserved Bongo samples were sub-sampled using a Folsom splitter where necessary, such that a minimum of 2000 particles were counted. Images were collected using a 5mm flow cell, a flow rate of 700 mL min^{-1} and an auto-image mode rate of 10 frames per second. Images were classified manually into broad taxonomic groups (cyclopoid copepods, small calanoid copepods, large calanoid copepods, *Rhincalanus gigas*, *Metridia* spp., polychaetes, gastropods, ostracods, appendicularians, euphausiids) to determine abundance using Visual spreadsheet software (Version 4.3.55). These data were used to calculate biomass by applying mass factors (Ward et al., 2012) to the abundance of each taxonomic entity (see supplementary table S1). Mass factors were calculated from published values (Ward et al., 2012) weighted by the relative abundance of the species within a taxonomic entity found in the Bongo net samples that were sent for taxonomic analysis. This had the effect of placing more emphasis on the taxa that dominate in the respective broad taxonomic groups.

2.2.3 Metabolic rates

One net of the Bongo catches was size fractionated (100-200 µm, 200-500 µm, 500-1000 µm, 1000-2000 µm, > 2000 µm) and frozen at -80 ^{o}C for later measurement of Electron Transport System (ETS) activity (Owens and King, 1975). During one station (P3C), a set of Bongo net samples taken from 0-75m, 75- 150m, 150-250m and 250-500m were frozen, without size fractionation, for measurement of the ETS activity of the total community. Separate Bongo deployments collected animals for grazing experiments, which were diluted in fresh seawater and immediately moved to a controlled temperature laboratory set to in situ surface temperature (2 ^{o}C).

Mammoth catches were frozen at -80 °C for later measurement of ETS activity of the >300 µm mesozooplankton community. A sub-sample of the dominant taxa found in the RMT catch was immediately flash frozen in liquid nitrogen and stored at -80 °C for later measurement of ETS activity. 10-40 replicate ETS samples were taken for each taxa.

2.3 Acoustic sampling

A multi-frequency (18, 38, 70, 120 and 200 kHz) drop-keel mounted echosounder (Simrad EK60) collected acoustic backscattering data (S_v, dB re $1m^{-1}$) throughout the cruise, where acoustic

backscatter is used as a proxy for mesozooplankton and micronekton biomass (depending on frequency). The echosounder was calibrated using standard sphere techniques (Demer et al., 2015) in Stromness Harbour, South Georgia on 27/11/2017. Raw data were collected to 1500 m at a ping rate of 3 seconds. Frequency specific mean values of sound speed (Mackenzie, 1981) and absorption coefficient (Francois and Garrison, 1982) were derived from CTD profiles for the typical depth ranges ensonified by each frequency, limited by the maximum depth of data used here (1000m, 1000m, 750m, 500m, 250m (18, 38, 70, 120 and 200 kHz respectively)). Data were processed in Echoview V10 (10.0.293.38183), this included: updating values of sound speed and absorption; cleaning noise (transient (set to -999 dB), intermittent (set to -999 dB) and background noise removed); removing periods when the vessel was on station (ship speed <2 knots); and resampling to then export S_v (dB re $1m^{-1}$) in cells of 1m vertical resolution and 1 minute horizontal. These data were allocated to day or night categories and further averaged to generate profiles of day and night distribution.

2.4 Respiration

2.4.1 Electron transport system (ETS) activity

To estimate respiration, we carried out ETS activity assays following the method of Owens and King (1975) with modifications from Gómez et al. (1996). Frozen specimens were reweighed in the laboratory. We used a weighed sub-sample, taken from just behind the head, for fish species caught by the RMT, whole individuals for other micronekton species, and the whole net sub-sample (split or size fraction) for mesozooplankton measurements. See Belcher et al. (2020) for further details about the specific mesopelagic fish respiration results.

Each sample was homogenised in a phosphate buffer, using either an electric homogeniser or a sonicator, for 30-60 seconds, before being centrifuged at 4000 rpm for 10 minutes at 0°C. 100 µL of the homogenate supernatant and 300 µL of reaction buffer (0.1 M, pH 8.5) containing substrates nicotinamide adenine dinucleotide (NADH) and nicotinamide adenine dinucleotide phosphate (NADPH) (saturating concentrations of 1.7 and 0.25 mM, respectively) were added to a semi-micro quartz cuvette. 100 µL 2-*p*-iodophenyl-3-*p*-nitrophenyl monotetrazolium chloride (INT, 4mM) was added to each cuvette to commence the reaction. All procedures were carried out on ice. The reaction was measured continuously for 8 minutes at a wavelength of 490 nm in a Cary 60 UV-Vis spectrophotometer (Packard and Christensen, 2004). The temperature of the reaction was controlled at 12 °C. To take into account the non-enzymatic reduction of INT (Maldonado et al.,

2012), a blank assay was also performed without ETS substrates for each sample. Reagent blanks were taken daily.

Formazan is produced during the kinetic assay as INT is reduced. INT takes the place of oxygen as the electron acceptor in the ETS, and accepts two electrons (oxygen would accept four). Therefore, the rate of formazan produced is related to oxygen consumption by a factor of two. Using the formazan production rate and our measured INT extinction coefficient (measured at 490 nm for each batch of INT; 13.3 - 16.4 mM^{-1} cm^{-1}) we calculated the potential respiration rate (Φ, µmol O_2 h^{-1}) following Packard and Christensen (2004). Using a conservative respiration to ETS (R:ETS) ratio of 0.5 (Ikeda, 1985; Hernández-León and Gómez, 1996), we then estimated the respiration at the experimental temperature of 12 °C. Where a subsample was taken (*i.e.* for fish), the total respiration rate per individual was calculated based on the ratio between the subsample and the total weight of the fish. To estimate the respiration rate at *in situ* temperatures, defined as the temperature from the CTD averaged over the net depth horizon, we used the Arrhenius equation and an activation energy of 62.8 kJ mol^{-1} (15 kcal mol^{-1}; Packard et al., 1975; Ariza et al., 2015; Hernández-León et al., 2019b). Respiration rates per hour were multiplied by 24 to give respiration rates per day, and a respiratory quotient of 0.9 was used to convert from oxygen to carbon (Ariza et al., 2015).

2.4.2 Mesozooplankton respiration

For the samples where we measured ETS activity, carbon specific respiration rates were calculated and applied to the biomass estimates from Bongo and MOCNESS samples described above and integrated over the volume filtered by the net to give daily respiration rates per m^3. WM of the ETS samples were converted to DM using a conversion factor of 0.25 (Kiørboe, 2013) and then to C using a conversion factor of 0.45 (Giering et al., 2019b). The carbon specific respiration (d^{-1}) of the equivalent Mammoth net was applied to the biomass from the MOCNESS net samples. For station P3B, where no Mammoth net ETS measurements were taken, the mean P3A and P3C specific respiration rates were applied. For the Bongo net, the carbon specific respiration (d^{-1}) of the appropriate size fraction was applied to each particle (based on area based diameter (ABD) measurements made by the FlowCam Macro) and summed for all particles in the Bongo sample.

2.4.3 Micronekton respiration

For the species where we measured ETS activity, we calculated allometric regressions (see supplementary table S2) relating WM (mg) to ETS-derived respiration ($\mu LO_2\ Ind^{-1}\ h^{-1)}$, with equations in the form of equation 2 where a_o and a_1 are constants:

$$\text{Ln (Respiration)} = a_o + a_1 \times \text{Ln (WM)} \qquad \text{(eq. 2)}$$

We found no significant relationship between ETS-derived respiration and WM for *E. triacantha*, and thus we used the mean measured respiration rate of 13.925 $\mu LO_2\ Ind^{-1}\ h^{-1}$.

It was not feasible to sample and conduct ETS assays on all species, thus we used allometric relationships from the literature to estimate respiration rates ($\mu LO_2\ Ind^{-1}\ h^{-1}$) for those species we were not able to measure (See Belcher et al., 2020 for a comparison of ETS and allometrically derived respiration in these samples). Taking the data from, and following the form of the regressions given in, Ikeda (2014), (equation 3 below), we calculated taxa specific linear regressions using multiple predictors (dry mass (DM, mg), temperature (T) and habitat depth (z, m)) with no interaction terms, where a_o, a_1, a_2 and a_3 are constants. See supplementary table S3 for allometric equations.

$$\text{Ln (Respiration)} = a_0 + a_1 \times \ln (\text{DM}) + a_2 \times 1000/T + a_3 \times \ln (z) \qquad \text{(eq. 3)}$$

For cephalopods, we used the data of Ikeda (2016) and carried out the same procedure as above but using body mass as WM.

Where allometric equations required DM, we made appropriate conversions using a combination of our own measurements from the DY086 research cruise where possible (supplementary table S4) and conversions from the literature (supplementary table S5). Once respiration rates per individual had been calculated, we summed them for each net deployment, and integrated over the volume filtered by the net to give respiration rates m^{-3}. For the RMT25 we summed all but the small euphausiid species (all euphausiids excluding *E. superba*), and we added this to the summed respiration of small euphausiids from the MOCNESS to give the total micronekton respiration. Respiration rates per hour were multiplied by 24 to give respiration rates per day, and a respiratory quotient of 0.9 was used to convert from oxygen to carbon.

2.4.4 Total community respiration

Total community respiration was summed over the coarsest depth ranges that samples were taken from, i.e. 0-250m and 250-500m sampled by the RMT25. MOCNESS nets aligned readily into this range (nets 2-5 = 250-500m, nets 6-9 = 0-250m). Bongo net samples, however, were taken from 0-150m and 150-500m. Bongo respiration per m^3 in 250-500m was assumed to be the same as that for

299 150-500m. Bongo respiration in 0-250m ($BR_{0\text{-}250}$, mmolC m^{-3} d^{-1}) was calculated as a weighted mean
300 of respiration rates for 0-150m ($BR_{0\text{-}150}$, mmolC m^{-3} d^{-1}) and 150-500m ($BR_{150\text{-}500}$, mmolC m^{-3} d^{-1})
301 (equation 4). Only respiration for Bongo net particles less than 300 µm were included to avoid
302 overlap with the MOCNESS respiration estimates.

303 $$BR_{0\text{-}250} = ((BR_{0\text{-}150} \times 150) + (BR_{150\text{-}500} \times 100))/250 \quad \text{(eq. 4)}$$

304

305 ***2.5 Ingestion***

306 ***2.5.1 Copepod grazing experiments***

307 All experimental work for grazing experiments was undertaken in a controlled temperature
308 laboratory set at in situ surface temperature (2 °C). Experimental animals were collected using a
309 motion-compensated Bongo net (100 µm mesh) using a non-filtering cod end (see section 2.1.1
310 above) and were sorted under dim light using a dissection microscope. Experimental water was
311 collected using Niskin bottles attached to a CTD rosette or a Marine Snow Catcher (Riley et al.,
312 2012). Incubations were carried out using water collected close to the subsurface chlorophyll
313 maximum, and with water collected from additional depths for *Oithona similis*. Copepod grazing
314 rates were examined using particle-removal experiments (Mayor et al., 2006). In brief, glass
315 incubation bottles were filled with un-screened seawater a little at a time to maximise homogeneity.
316 Visibly discernible copepods were removed from the incubation bottle via a dip-tube. Experimental
317 animals were carefully introduced into bottles and incubated in triplicate alongside triplicate control
318 bottles in the dark on a plankton wheel rotating at 1 rpm for 24 hr and were terminated by adding
319 1% acidified Lugol's iodine. Microplankton samples (200 mL) from the start of the experiment and
320 from each of the incubated bottles were collected and preserved with acidified Lugol's iodine (1%).
321 Experiments were conducted for dominant copepod species that represented different functional
322 feeding types in the copepod community: small particle associated copepods (*Oithona similis*), small
323 (*Ctenocalanus* spp.), intermediate (*Calanoides acutus*) and large filter-feeding copepods
324 (*Rhincalanus gigas*), strongly migrating copepods (*Metridia* spp.). See Table 2 for a summary of
325 experiments. Copepod mortality in experiments ranged from 0-26% (mean 9%).

326 The concentrations of different cell types in 5 mL of the preserved microplankton samples were
327 counted using a FlowCam 8400 (Yokogawa Fluid Imaging Technologies Inc.) fitted with a 10x
328 objective and a FOV100 flow cell, at a flow rate of 0.25 mL min^{-1}. Images were collected using auto-
329 image mode at a rate of 37 frames per second. For the experiment using water collected at 350m,
330 where particle concentrations were low compared to the surface, samples were settled for 48 hours,

and reduced to 50% of the original volume before analysis. Libraries of dominant cell types were created and used in conjunction with size filters to classify particles automatically into broad taxonomic groups (flagellates, small dinoflagellates, large athecate dinoflagellates, large thecate dinoflagellates, ciliates, pennate diatoms, centric diatoms and unidentified cells) using Visual spreadsheet software (Version 4.3.55). Automatic classifications were checked manually, and corrected when necessary (~ 50% of particles). Biomass (µg C) was calculated using particle volume (μm^3) and published carbon to volume relationships (Alldredge, 1998; Menden-Deuer and Lessard, 2000). Ingestion rates were calculated using the equations of Frost (1972) and converted to carbon specific ingestion rates using published estimates of copepod's biomass (Ward et al., 2012).

Table 2: Summary of copepod grazing experiments

Species	Station	Stage	No. animals	Incubation vol (L)	Water collection depth (m)	Average % cells remaining
Oithona similis (applied to cyclopoid and harpacticoid copepods)	P3A	CV-CVI	20	0.2	20	80
		CV-CVI	20	0.2	350	89
	P3B	CIII-IV	20	0.2	30	80
	P3C	CV-CVI	20	0.2	75	88
		CIII-IV	30	0.2	75	86
Calanoides acutus (applied to *Calanus* spp.)	P3A	CIV-CV	5	1.1	30	94
	P3B	CV	7	1.1	30	94
	P3C	CV	5	1.1	30	79
Rhincalanus gigas	P3A	CVI	1	1.1	30	88
	P3B	CVI	1	1.1	30	95
	P3C	CVI	1	1.1	30	85
Ctenocalanus spp. (applied to small calanoid copepods)	P3A	CV-CVI	20	1.1	30	87

Metridia spp. (applied to Metridinidae and Euchaetidae)	P3B	CVI	8	1.1	30	80

342

343 ***2.5.2 Total community ingestion***

344 Carbon specific ingestion rates (d^{-1}) were applied to the biomass of appropriate taxa from net
345 samples to calculate total daily ingestion rates m^{-3}. For *Oithona*, ingestion rates measured using
346 deep water were applied to deep nets; for all other taxa we applied ingestion rates measured using
347 surface water throughout the water column. As we could not feasibly measure ingestion rates for all
348 species, measured copepod specific ingestion rates (see above) were applied to the biomass of other
349 copepods sharing similar body size and feeding traits (Table 2). Published values for specific
350 ingestion rates (daily ration), measured in polar and sub-polar regions, were used for species or
351 groups from Bongo, MOCNESS and RMT25 samples for which we did not measure ingestion (see
352 supplementary table S6). Since the mesopelagic fish community in the Scotia Sea is dominated by
353 myctophids and bathylagids (Collins et al., 2012) we applied a single daily ration to all fish species. A
354 daily ration of 3% was used for categories for which there was no suitable data available in the
355 literature (appendicularians, barnacle nauplii, carnivorous copepods such as Euchaetidae, cnidarians,
356 gastropods, isopods, mysids, cladocerans and polychaetes) based on the mean of the other compiled
357 data (see supplementary table S6, excluding *Oithona similis* and *Salpa thomsoni* which had daily
358 rations > 20%). Only ingestion for Bongo net particles less than 300 µm were included to avoid
359 overlap with the MOCNESS ingestion estimates.

360

361 ***2.6 Lipid analysis***

362 *Calanoides acutus* C5 and *Rhincalanus gigas* C6 female lipid extractions were carried out on each
363 homogenised freeze-dried (-60°C; 10^{-2} mBar) sample (1 – 60mg). An internal standard (30-100 µL of
364 5α(H)-cholestane; 101 ng μL^{-1}) was added to each sample, followed by a mixture of dichloromethane
365 (DCM) and methanol (9:1; 15 mL). The samples were then sonicated (15 min, x2) and the resulting
366 extract was decanted into round bottom flasks. The solvent obtained was evaporated to dryness
367 under vacuum using a rotary evaporator at ~30°C. Each sample was then passed through a Pasteur
368 pipette filled with anhydrous sodium sulphate using DCM (3 mL). The solvent was blown down with

nitrogen gas and the samples were stored (-20°C) before transmethylation and derivatisation with BSTFA.

GC-MS analyses were conducted using a GC Trace 1300 fitted with a split-splitless injector and column DB-5MS (60m x 0.25mm (i.d.), with film thickness 0.1 μm, non-polar stationary phase of 5% phenyl and 95% methyl silicone), using helium as a carrier gas (2 mL min^{-1}). The GC oven was programmed after 1 minute from 60°C to 170°C at 6°C min^{-1}, then from 170°C to 315°C at 2.5 °C min^{-1} and held at 315 °C for 15 min. The eluent from the GC was transferred directly via a transfer line (320°C) to the electron impact source of a Thermoquest ISQMS single quadrupole mass spectrometer. Typical operating conditions were: ionisation potential 70 eV; source temperature 215°C; trap current 300 μA. Mass data was collected at a resolution of 600, cycling every second from 50– 600 Daltons and were processed using Xcalibur software.

Compounds were identified either by comparison of their mass spectra and relative retention indices with those available in the literature and/or by comparison with authentic standards. Quantitative data were calculated by comparison of peak areas of the internal standard with those of the compounds of interest, using the total ion current (TIC) chromatogram. The relative response factors of the analytes were determined individually for 36 representative fatty acids, sterols and an alkenone using authentic standards. Response factors for analytes where standards were unavailable were assumed to be identical to those of available compounds of the same class.

2.7 Data analysis

Given the inherent patchiness in zooplankton and micronekton distribution and abundance, we have limited the statistical analyses of these complex communities and therefore do not extend our conclusions beyond the data available. The total biomass of mesozooplankton and micronekton did not change from P3A to P3C suggesting that our measurements can be treated as replicate occupations of station P3 rather than separate stations. Wilcoxon rank sum tests were used to test whether the total lipid content of *C. acutus* and *R. gigas* changed between stations P3B and P3C. Spearman's correlation was used to test whether total pelagic community respiration and ingestion rates were correlated.

3 Results

Detailed description of the sampling environment can be found in Ainsworth et al. (2023) and Giering et al. (2023). In brief, there were deeper mixed layers during P3A and P3B (70m) compared to P3C (60m). Water column temperature was fairly consistent (surface = 2.3-3.6 °C, upper mesopelagic = 0.8-1.5 °C). Surface chlorophyll concentration decreased from station P3A to P3C, but remained high throughout the sampling period (>1mg m^{-3}) (Ainsworth et al., 2023). The subsurface chlorophyll depth (mean = 32 ± 14m) and concentration (mean = 3.5 ± 1.8 mgm^{-3}) were variable, even within stations. POC concentrations at the surface declined from station P3A to P3C, whilst concentrations in the upper mesopelagic increased during this time (Giering et al., 2023). Mean day length was 16 hours ± 30 minutes and lunar phase was 'new' during P3A, 'full' during P3B and 'last quarter' during P3C.

3.1 Biomass

The greatest concentration of biomass, by three orders of magnitude, was found in mesozooplankton samples taken by the MOCNESS (>330 µm). The ranges of biomass found in Bongo net (>100 µm), MOCNESS (>330 µm) and RMT25 (>4 mm) samples were 0.08-0.13, 17.9-47.1 and 0.11-1.19 mmolC m^{-3} (0.96-1.62, 214.8-565.1 and 1.38-2.27 mgC m^{-3}) respectively; hereafter biomass data are given in molar units of carbon. The biomass in Bongo net samples was dominated by large copepods and polychaetes (predominantly *Pelagobia* spp.) at both depths (Figure 1). The surface MOCNESS samples were dominated by *Calanoides acutus* stages C4-5 (mean 74% of total biomass from the MOCNESS, Figure 1). In the rest of the water column *C. acutus* C4-5 and *Rhincalanus gigas* C6 females constituted a mean 32-43% of total biomass from the MOCNESS. The remainder of the biomass was made up of a number of different species which individually contributed < 5% to the total biomass. Mesopelagic *Bathylagus* spp., myctophids (*Krefftichthys anderssoni*, *Gymnoscopelus braueri*, *Electrona antarctica* and *Protomyctophum tenesoni*), other fish and euphausiids formed >80% of the biomass from RMT25 nets, with the fish being more dominant in the deeper samples (Figure 1). There were no obvious changes to the broad taxonomic composition of mesozooplankton and micronekton biomass over the duration of the cruise.

The total biomass of mesozooplankton and micronekton did not change from P3A to P3C (Figure 2). Day/night profiles of total mesozooplankton and micronekton biomass showed no consistent evidence of synchronised DVM (Figure 2, Supplementary figures 1 and 2). The biomass at night ranged between 28-183% of that during the day, with a mean of 95.2 $\pm$ 63.2%. In general, there was greater biomass in the surface samples compared to deeper samples during both the day and night. The change in weighted mean depth (ΔWMD) between day and night was <50 m for total biomass of

mesozooplankton from the MOCNESS net and micronekton from the RMT25 net (Figure 3), with no consistency in whether total biomass was deeper or shallower during the day. When considering specific taxa, there were consistent depth changes for appendicularians (shallower during the day by < 50m), *Metridia* spp. (deeper during the day by 20-110m), salps (deeper during the day by 50-140m), bathylagids, myctophids and other fish (deeper during the day by 50-115m) and decapods (deeper during the day by 10-110m).

Vertical profiles of acoustic backscatter at 18 and 38 kHz (indicating fish and micronekton) showed little or no evidence of synchronised DVM of the deep scattering layers (e.g. 250 m, 450 m and 700m) during P3A and P3B, although there was greater biomass at night in the top 50m compared to the day (supplementary figures S1 and S2). There was evidence for day/night differences in the top 125 m of the water column in the higher frequency profiles of 120 and 200 kHz (indicating copepods and smaller euphausiids). In general, there was more backscatter in surface waters at night, but it was not possible to discern which depth it had originated.

3.2 Respiration

Mean (± s.d.) mesozooplankton daily carbon specific respiration rates at in situ temperatures 0.9-3.2 °C were 0.96 ± 0.77 % d^{-1}. For comparison with wider literature we calculate respiration rates at 20 °C, using a standard Q_{10} of 2 (although see Maas et al., 2021), giving a mean (± s.d.) mesozooplankton daily specific respiration rate at 20 °C of 3.3 ± 2.5 % d^{-1}. Specific respiration at the *in situ* temperature in Bongo net samples during P3C ranged between 0.15 and 0.95 % d^{-1}. Specific respiration rates in Mammoth samples at the *in situ* temperature were higher during P3C (0.31-3.8 % d^{-1}) than P3A (0.10-1.7 % d^{-1}). Carbon specific respiration rates were highest in surface samples, decreased with depth to a minimum at around 400m, and were on average 9% higher during the day compared to the night (Supplementary figure S3).

Total community respiration in Bongo (>100 µm), MOCNESS (>330 µm) and RMT25 (>4 mm) net samples ranged between 0.03-0.09, 0.31-1.40 and 0.002-0.02 mmolC m^{-3} d^{-1} (0.34-1.04, 3.69-16.81 and 0.02-0.20 mgC m^{-3} d^{-1}) respectively. Pelagic respiration (mmolC m^{-3} d^{-1}) was dominated by the >330 µm mesozooplankton from the MOCNESS samples (Figure 4) and was higher in surface samples compared to deeper samples from all net types. Total mesozooplankton respiration was higher during P3C compared to the other stations in Bongo (maximum 0.02, 0.02, 0.07 mmolC m^{-3} d^{-1} during P3A, B, C respectively) and MOCNESS (maximum 0.24, 1.33 mmolC$m^{-3}d^{-1}$ during P3B, C respectively) mesozooplankton samples. Micronekton respiration from the RMT25 samples was dominated by

euphausiid respiration but was very low compared to mesozooplankton respiration. Micronekton respiration was lowest during P3A (maximum 0.0008 mmolCm^{-3}d^{-1}; 0.01 mgC m^{-3} d^{-1}), highest during P3B (maximum 0.01 mmolCm^{-3}d^{-1}; 0.18 mgC m^{-3} d^{-1}) and was always higher at night compared to the day.

3.3 Ingestion

The phytoplankton community in the experimental incubation water collected from the surface was dominated by diatoms larger than 10 µm (*Chaetoceros* spp., *Thalassionema nitzschioides*, *Fragilariopsis kerguelensis*, *Eucampia antarctica*, and *Pseudo-nitzschia* spp.) throughout the study period with cell counts > 500 cells mL^{-1} (Ainsworth et al., 2023). This was also apparent in the experimental incubation water collected from the surface (Supplementary figure S4A), but deep incubation water was dominated by flagellates and unidentified particulate matter.

Carbon specific ingestion rates measured ranged between 0.13-145 % d^{-1}. Mean carbon specific ingestion rates of *O. similis* were always high compared to the other copepod species measured (Supplementary figure S4B, supplementary table S6) and were on average three times higher in younger *O. similis* stages (C3-4: 55.4-145.9 % d^{-1}) compared to older stages (C5-6: 2.4-59.0 % d^{-1}). *Ctenocalanus* spp. and *Metridia* spp. had intermediate carbon specific ingestion rates (7.7-11.2 and 5.1-10.6 % d^{-1} respectively), whilst *C. acutus* and *R. gigas* consistently had low carbon specific ingestion rates (0.1-2.3 and 0.4-7.7 % d^{-1} respectively).

Oithona similis (all stages measured) incubated in water collected from the chlorophyll maximum ingested a high percentage of unidentified cells (45.4-59.1% of total carbon ingested) which was largely made up of phytodetritus, faecal pellets and aggregates (Supplementary figure S4A). The rest of their diet was a mix of diatoms and dinoflagellates, with some ciliates. The only exception to this was during P3A for *O. similis* incubated in water collected at the surface, where 86.9% of the diet was diatoms. *O. similis* incubated with water collected at 350m ingested unidentified cells (66.7%) and ciliates (25.0%). Diatoms were the largest component of the diet for all *C. acutus* (45.4-60.9%), *R. gigas* (37.5-70.0%) and *Ctenocalanus* spp. (48.7%) (Supplementary figure S4A). For both *C. acutus* and *R. gigas,* the rest of the diet was mainly composed of ciliates during P3B (31.4% and 24.7% respectively) and dinoflagellates during P3C (28.0% and 24.9% respectively). The diet of *Metridia* spp. was fairly evenly split between diatoms (35.2%), dinoflagellates (28.0%) and ciliates (32.7%) (Supplementary figure S4A). There were few consistent patterns in feeding selectivity, however *O. similis* tended to select against large thecate dinoflagellates preferring ciliates and phytodetrital

aggregates whilst all other copepods selected for large thecate dinoflagellates and against phytodetrital aggregates.

Total community ingestion in Bongo net (>100 µm), MOCNESS (>330 µm) and RMT25 (>4 mm) samples ranged between 0.0003-0.0007, 0.53-1.30, 0.004-0.010 mmolC m^{-3} d^{-1} (0.003-0.009, 6.34-15.63 and 0.05-0.12 mgC m^{-3} d^{-1}) respectively. Pelagic ingestion was dominated by that of mesozooplankton >330 µm from the MOCNESS samples (Figure 5). Total ingestion from these MOCNESS samples was always higher in surface samples compared to deep samples reflecting the higher biomass in these nets. There was no substantial change in ingestion rates over time.

3.4 Lipid content

The total lipid content (mg total lipid per g organic carbon (OC)) of *C. acutus* changed from 924.1 ± 233.9 to 785.1 ± 232.5 mg g^{-1} OC between P3B (n=3) and P3C (n=3), respectively, although this decrease was not significant (Wilcoxon rank sum test, W = 6, p = 0.35, Table 4). For *R. gigas* however, there was a significant decrease in total lipid content from 798.1 ± 138.0 to 500.1 ± 51.3 mg g^{-1} OC between P3B (n=4) and P3C (n=3), respectively (Wilcoxon rank sum test, W = 12, $p < 0.05$, Table 3).

Table 3: Total lipid content (mg total lipid per g organic carbon (OC)) of copepods *Calanoides acutus* stage C5 and *Rhincalanus gigas* stage C6 female collected from MOCNESS tows during stations P3B and P3C.

Species	Station	MOCNESS Event	Depth	Total lipid content (mg g^{-1} OC)
Calanoides acutus C5	P3B	217	0-62m	918.6
		234	187-250m	693.0
		217	437-500m	1160.7
	P3C	315	0-62m	1045.1
		315	125-187m	597.3
		315	375-437m	712.8
Rhincalanus gigas C6F	P3B	234	0-62m	612.7
		217	187-250m	928.0
		217	250-312m	779.4
		234	375-437m	872.3
	P3C	315	125-187m	539.3
		315	250-312m	518.9
		315	375-437m	442.1

3.5 Carbon budgets of the mesopelagic zooplankton and nekton communities in the Scotia Sea

Total pelagic community respiration and ingestion rates were within the same order of magnitude (Figure 6) and were highly positively correlated (Spearman correlation $r = 0.81$, $p < 0.05$, $N = 16$). These metabolic rates did not vary with station or time of day in deep samples where ingestion rates were always higher than respiration rates (mean ingestion = 0.08 ± 0.009 mmolC m^{-3} d^{-1}, mean respiration = 0.02 ± 0.001 mmolC m^{-3} d^{-1}). There was higher variability in the metabolic rates from shallow samples. Rates were lower during P3B (mean ingestion = 0.54 ± 0.02 mmolC m^{-3} d^{-1}, mean respiration = 0.58 ± 0.08 mmolC m^{-3} d^{-1}), than during P3C (mean ingestion = 0.84 ± 0.55 mmolC m^{-3} d^{-1}, mean respiration = 0.84 ± 0.77 mmolC m^{-3} d^{-1}). Though there was no consistent day/night change during P3B, the daytime metabolic rates during P3C were 3-5 times higher than those during the night. Respiration rates were only lower than ingestion rates in shallow samples on one occasion.

4 Discussion

Quantifying the vertical distribution and movements of zooplankton, along with their feeding behaviours and metabolic requirements, is integral to understanding how ocean biology contributes to the biological carbon pump (Steinberg and Landry, 2017). We quantified the magnitude of diel vertical migration (DVM) and physiological rates of mesozooplankton and micronekton communities off South Georgia in the Scotia Sea (S. Atlantic) in order to contribute to a synthesis of the mesopelagic carbon budget at this site (Giering et al., 2023). There was an apparent excess of ingested carbon relative to metabolic requirements in the deep samples, but total community respiration was greater than ingestion for most shallow samples suggesting a potential metabolic imbalance in surface waters consistent with the observation that flux attenuation was greater than POC accumulation in the shallow mesopelagic (Giering et al., 2023).

4.1 Biomass and DVM

Total integrated biomass estimates, for stations where there was a complete suite of net measurements (Figure 2), were towards the high end of previous estimates in the same area (Ward et al., 2012) The biomass dominance of intermediate and large calanoid copepods (*Calanoides acutus* and *Rhincalanus gigas*) in the mesozooplankton, and euphausiids, bathylagid and myctophid fish in the micronekton (Figure 1) is also consistent with the literature (e.g. Atkinson et al., 2012; Collins et al., 2012; Ward et al., 2012).

We found little evidence of any synchronised DVM at the population level using the biomass data (Figures 2-3). This may be consistent with the satiation sinking hypothesis (Tarling and Johnson, 2006; Tarling and Thorpe, 2017), where individuals asynchronously swim to the surface to feed and passively sink once satiated. The bulk of the mesozooplankton/micronekton biomass was consistently found in the top 62 m except for taxa that underwent synchronised DVM (*Metridia* spp., salps, bathylagids, myctophids, other fish and decapods). The acoustics data (supplementary figures S1-2) also provided little evidence of synchronised DVM in the fish and large micronekton (as evidenced by the 18 and 38 kHz). It is possible that vertical migration was still taking place in an unsynchronised manner over the day night cycle, but this was not resolved by the techniques available to us during the present study.

DVM is a behavioural response to a combination of exogenous factors (e.g., light, temperature, salinity, and oxygen) and endogenous factors (e.g. sex, age, satiation, and physiology) (Forward, 1988) thought to maximise feeding opportunities whilst minimising predation risk (e.g. De Robertis, 2002; Hansen and Visser, 2016). Studies in the Antarctic have shown variable presence of DVM (e.g. Conroy et al., 2020; Kwong et al., 2020 and references therein) and it has been proposed that phytoplankton blooms can halt DVM (Cisewski et al., 2010; Cisewski and Strass, 2016) or that the apparent lack of DVM can result from not sampling the right depths (Flores et al., 2014). Omand et al. (2021) recently reported upward migrations of animals at ~300m driven by cloud shadows which could also have impacted behaviours during our study (Platnick et al., 2015). In the case of the lipid-storing copepod species, *C. acutus*, which dominated the mesozooplankton biomass, the absence of synchronised DVM may also indicate that a proportion of their population was still in the process of emerging from diapause. This is consistent with the observed phenology of *C. acutus* in the vicinity of our sampling location (supplementary figure S5), where animals typically exit diapause between November and December. However, at the community scale, it seems most likely that the lack of synchronised DVM was due to the excellent feeding conditions in the surface waters and resulting high levels of high quality POM throughout the water column (Giering et al., 2023) as has previously been observed during spring blooms in the Lazarev and Weddell seas (Cisewski et al., 2010; Cisewski and Strass, 2016).

One of the challenges for identifying patterns of synchronised DVM in micronekton and particularly myctophid fish is active net avoidance (Kaartvedt et al., 2012) and the depth at which they reside during the day (>500m; Cotté et al., 2022). Many studies use only night time nets to determine fish biomass (e.g. Collins et al., 2012), noting that daytime avoidance of pelagic nets is common and biases our understanding of DVM. It should also be noted that our nets were limited to the top 500 m of the water column, and DVM can occur at depths greater than this. However, whilst scattering

582 layers were observed below 500 m at 700m water depth, there was also no evidence of day/night
583 differences in the intensity or depth of these layers indicating limited migration to shallower waters.

584

585 ***4.2 Physiological rates***

586 Temperature-corrected (to 20 °C using Q_{10} = 2, see section 3.3) daily carbon specific respiration rates
587 for mesozooplankton were consistent with published values and showed a decrease with depth, as
588 reported previously (Steinberg et al., 2000; Ikeda et al., 2006; Yebra et al., 2018; Hernández-León et
589 al., 2019a; Hernández-León et al., 2019c; Landry et al., 2020). Exactly what drives this apparently
590 common trend is unclear. The temperature-dependence of their respiration rates (Ikeda, 1985;
591 Ikeda, 2014) provides a potential explanation, although the lack of a clear relationship between
592 water temperature and specific respiration (Supplementary figure S3) suggests that this is not the
593 only driver. Belcher et al. (2020) similarly found that temperature was a less significant driver of
594 respiration rates over the small temperature range found in the Scotia Sea compared to areas with
595 larger temperature gradients. Specific respiration rates also scale as a function of biomass, with
596 larger animals having lower rates than their smaller counterparts (e.g. Kiørboe and Hirst, 2014). The
597 biomass in our surface nets was dominated by the intermediate-sized (~30 µmol C copepod^{-1}) *C.*
598 *acutus*, whereas the deeper nets showed increasing contributions of the far larger (~88.3 µmol C
599 copepod^{-1}) *R. gigas*. This shift towards an increasing contribution of large copepods at greater
600 depths is generally consistent with the idea that the observed decrease in specific respiration rates
601 may be attributable to a shift in the size structure of the zooplankton community. An additional,
602 non-mutually exclusive explanation for the decline with specific respiration with depth is that an
603 increasing fraction of both *R. gigas* and *C. acutus* in the deeper nets were still in, or in the process of
604 emerging from, diapause, during which respiration rates are significantly lower (Hirche, 1984; Drits
605 et al., 1994; supplementary figure S5). Unfortunately, our ETS-based estimates of respiration in the
606 MOCNESS nets, where these species dominated, were generated using bulk community samples,
607 and therefore it is not possible to explore this idea further.

608 Total respiration rates in the deep samples (0.015-0.018 mmolC m^{-3} d^{-1}; 0.18-0.22 mgC m^{-3} d^{-1}, Figure
609 4) were also comparable to previous studies using direct measurements, e.g. 0.014-0.067 mmolC m^{-3}
610 d^{-1} (0.17-0.80 mgC m^{-3} d^{-1}) in the SW Mediterranean (Yebra et al., 2018) and 0.024-0.051 mmolC m^{-3}
611 d^{-1} (0.29-0.62 mgC m^{-3} d^{-1}) in the Southern Ocean (Mayzaud et al., 2002b). By contrast, total
612 respiration rates in surface samples (0.29-1.38 mmolC m^{-3} d^{-1}; 3.52-16.6 mgC m^{-3} d^{-1}, Figure 4) were
613 at least an order of magnitude higher than previous studies, although we recognise that published
614 rates vary considerably depending on the methods employed (Hernández-León and Gómez, 1996;

Hernández-León and Ikeda, 2005; Bondyale-Juez et al., 2017; Belcher et al., 2020). We estimated respiration using a combination of allometric equations and ETS assays, both of which will have introduced a number of uncertainties beyond those associated with methods employed to generate the underlying estimates of biomass. For example, R:ETS ratios in the literature range from 0.16 to 2.55 (Hernández-León and Gómez, 1996; Osma et al., 2016a; Osma et al., 2016b; Bondyale-Juez et al., 2017), although ratios measured in the laboratory with cultured animals are rarely >1. We used a fixed R:ETS ratio of 0.5, which is considered conservative (Ikeda, 1985; Hernández-León and Gómez, 1996), and assumed constant respiration during day and night. However, Belcher et al. (2020) calculated an R:ETS ratio of 0.14 for the mesopelagic fish the Scotia Sea (based on ETS measurements and allometrically derived respiration rates) so it may be that 0.5 is excessive. An R:ETS ration of 0.14 would result in a 72% decrease in estimated respiration if applied to all taxa, or a 2-40% decrease in estimated micronekton (RMT) respiration if applied only to fish. In addition, Belcher et al. (Belcher et al., 2019b) found notable variability in therespiration rates of mesopelagic fish in the Scotia Sea which was not apparent in allometrically-based estimates, suggesting that allometric estimates may not capture the true scale of variability which could introduce errors that propagate when generating population-scale estimates. We converted estimated values of oxygen consumption into carbon units using a fixed RQ of 0.9, based on the assumption that the sampled animals were respiring proteins and carbohydrates (Prosser, 1961). However, the prevalence of *C. acutus* stage 5 copepodites with substantial lipid reserves throughout the water column (Figure 1, Table 3) suggests that a proportion of the community was emerging from diapause and thus still using lipid-based metabolism. In this case, an RQ of ~0.7 may have been more appropriate (Prosser, 1961), and therefore our assumed value of RQ = 0.9 would have overestimated respiration rates considerably (see Section 4.3, below).

Daily specific ingestion rates of the copepod species examined generally agreed well with previous studies, although rates for *C. acutus* were towards the lower end of published values (Atkinson et al., 1992; Atkinson et al., 1996; Swadling et al., 1997; Hernández-León et al., 2000; Bernard and Froneman, 2003; Sarthou et al., 2008). The highest specific ingestion rates were found in the smaller species, e.g. *Oithona similis* and lowest in the largest (*Rhincalanus gigas*), consistent with metabolic scaling theory (Kiørboe and Hirst, 2014). The low ingestion rates for *C. acutus* stage C5 may again be because many of these individuals were still in the process of breaking the winter dormancy, although low ingestion rates for this species are not uncommon (e.g. Drits et al., 1994; Mayzaud et al., 2002a). Patterns in feeding selectivity were also consistent with those in the literature, with *Oithona* spp. and *Metridia* spp. showing preference for motile prey, and *C. acutus* and *R. gigas* feeding mainly on diatoms (Atkinson, 1995; Atkinson et al., 2012). Our results also suggest that

649 *Oithona* spp. fed substantially on phytodetritus, faecal pellets and aggregates (the 'unidentified
650 particles' category) which represented ~50% of their total diet. These types of particles cannot
651 easily be counted using microscopy with settled samples, the traditional way of enumerating cells in
652 particle removal grazing experiments. The FlowCam however can count these particles and provides
653 an image for each, which can be used as a means to estimate volume and subsequently carbon
654 content. Including these particles in grazing estimates does, however, introduce caveats. In the
655 absence of alternative information, we used a single volume to carbon relationship for phytodetrital
656 aggregates to estimate the carbon content in all unidentified particles. It is possible that this could
657 both over-estimate (e.g. aggregates dominated by empty diatom frustules) and under-estimate (e.g.
658 aggregates containing live dinoflagellates) the carbon content of such particles. Particle
659 fragmentation by these and other particle-associated copepods has been proposed as an important
660 mechanism for supporting their nutritional requirements (Mayor et al., 2014) and attenuating
661 sinking flux in the mesopelagic (Mayor et al., 2020). Therefore these 'unidentified particles' could
662 result from copepod feeding behaviour during the incubations causing particle disaggregation. By
663 contrast, rotation of bottles on the plankton wheel could have led to the aggregation of smaller
664 particles into larger ones over the duration of the incubations, with any such effects differing
665 between the control and experimental bottles if the incubated copepods were fragmenting particles.
666 More detailed observations of how small, particle-associated copepods interact with particles,
667 alongside a better understanding of how particle composition relates to its elemental and
668 biochemical composition, are clear priorities for future mesopelagic research (Koski et al., 2017;
669 Koski et al., 2020; Mayor et al., 2020).

670 As for total respiration, total ingestion rates in deep samples (250 – 500m; Figure 5; Table 4) were
671 comparable to previous studies (Swadling et al., 1997; Mayzaud et al., 2002b; Pakhomov et al.,
672 2002). Total community ingestion rates in surface samples (0 – 250m; Figure 5; Table 4) were at
673 least an order of magnitude higher than those in deep samples and were more comparable to
674 maximum rates found in Antarctic coastal waters (Swadling et al., 1997). When calculating ingestion
675 rates, we assumed that animals were feeding at depth since we found no clear evidence of
676 synchronised DVM and significant flagellate concentrations were observed at 350m (Supplementary
677 figure S4A). We applied the same biomass-specific ingestion rate to surface and deep biomass
678 measurements which may have resulted in an overestimation of the total community ingestion over
679 the water column since most ingestion experiments used water collected from near surface. We did
680 quantify ingestion rates for *Oithona* spp. incubated with water collected at depth (350m) and found
681 slightly lower mean specific ingestion rates compared to surface waters (Supplementary figure S4B).

682

4.3 Metabolic budgets

Total mesozooplankton and micronekton community respiration and total ingestion estimates were always within the same order of magnitude. Respiration accounted for between 17.0-23.5% of the total ingested carbon in the deep samples (Table 4), suggesting that the food ingested was more than sufficient to meet the observed metabolic requirements. The apparent excess of ingested carbon relative to respiratory requirements at depth supports the observation that food (POM) quality is poor in the mesopelagic relative to the mixed layer (based on the relative concentrations of polyunsaturated fatty acids; C. Preece and G. Wolff, personal communication), and organisms therefore have to consume a larger quantity of food in order to fulfil their metabolic and nutritional requirements (Giering et al., 2014; Mayor et al., 2014; Anderson et al., 2017; Mayor et al., 2020).

Ingested C needs to be sufficient to simultaneously fuel respiration, growth/reproduction and excretion/egestion so, at steady state, should be substantially higher than the respired C alone. During the night visit to P3C, the estimated total respiratory demand of the surface community was again below the total amount of carbon ingested (respiration = 64.2% of ingested carbon; Table 4), leaving an apparent metabolic deficit. Carbon absorption efficiencies in copepods are reported to range between ~35-90% (Mayor et al., 2011 and Supplementary Table S3 therein), indicating that although the night surface population during P3C had consumed sufficient food to meet their respiratory demands, there was little excess to support an actively growing population. By contrast, respiration was greater than or equal to ingestion for all other shallow samples (respiration = 100-117% of ingestion; Table 4). This surprising result is, in fact, consistent with several other studies, where respiration is reported to be up to ~ 400% of ingestion (e.g. Atkinson, 1996; Razouls et al., 1998; Mayzaud et al., 2002b). Such discrepancies have previously been attributed to the absence of sufficient prey and the consumption of non-phytoplankton material. However, neither of these explanations appear appropriate in our study, owing to the high concentrations of particles throughout the water column (Giering et al., 2023) and our attempts to quantify the removal of all cell types, including both microzooplankton and detrital particles. These results may therefore suggest that our estimated rates of respiration were excessive, or that an alternative carbon source was available.

The lipid-rich copepods, *C. acutus* and *R. gigas*, constituted between ~40-80% of the total mesozooplankton biomass in the shallow nets (Figure 1), and considering that our sampling coincided with the period during which these animals exit diapause (supplementary figure S5), it seems likely that the apparent discrepancy between estimated total community rates of respiration and ingestion can be at least partially attributed to these animals being somewhat reliant upon the

consumption of internal lipid stores. The total lipid content of *C. acutus* and *R. gigas* decreased between P3B and P3C, although this decrease was only significant for *R. gigas*. This would simultaneously explain the low ingestion rates of these animals and produce an overestimate of respiration using our assumed RQ = 0.9. Indeed, recalculating total community respiration with an RQ of 0.7, ingestion was greater than respiration in all samples, although, in some cases, a high absorption efficiency (>90%) must be implied for there to be enough carbon to meet respiratory demands (Table 4). It should be noted, however, that our observations relate specifically to the community at P3 in spring, and may not be representative of annual carbon budgets or of those elsewhere in the Southern Ocean.

Table 4: P3 metabolic budgets. Estimated total mesozooplankton and micronekton community rates of respiration (R, mmolC m^{-3} d^{-1}), calculated using respiratory quotients (RQ) of 0.9 and 0.7, and ingestion (I, mmolC m^{-3} d^{-1}).

			P3B		P3C	
			250-350	0-250	250-500	0-250
R (mmolC m^{-3} d^{-1})	RQ=0.9	Night	0.016	0.64	0.017	0.29
		Day	0.015	0.52	0.018	1.38
	RQ=0.7	Night	0.013	0.50	0.013	0.23
		Day	0.012	0.41	0.015	1.10
I (mmolC m^{-3} d^{-1})		Night	0.095	0.55	0.076	0.46
		Day	0.089	0.52	0.078	1.23
R:I	RQ=0.9	Night	0.17	1.17	0.22	0.64
		Day	0.17	1.00	0.24	1.13
	RQ=0.7	Night	0.14	0.91	0.17	0.50
		Day	0.13	0.78	0.19	0.88

4.4 Conclusions

Synchronised Diel Vertical Migration (DVM) should not be assumed, even for taxa previously shown to undertake the behaviour. This study did not observe synchronised DVM in either total biomass or in the majority of taxa examined. This lack of synchronised DVM patterns may be due to the fact that sampling took place during mid-spring when feeding conditions in the upper 200m were good.

Nevertheless, our findings do not exclude the possibility that asynchronous vertical migration was taking place during this time.

The apparent excess of ingested carbon relative to respiratory requirements in the deep mesopelagic samples supports the understanding that food quality below 200m is poor and organisms have to consume a larger quantity of food in order to fulfil their metabolic and nutritional requirements. Our results also suggest that *Oithona* spp. fed on phytodetritus, faecal pellets and aggregates. These results are consistent with particle fragmentation by copepods and microbial gardening hypotheses, which could therefore play an important role in attenuating carbon flux.

There is a need to better understand the physiology of shallow water animals when assessing carbon budgets, particularly where lipid-storing species predominate. For shallow samples, we found that ingestion rates could support respiratory demands if, when calculating total community respiration, we used an RQ of 0.7, appropriate for animals respiring lipid, rather than an RQ of 0.9, appropriate for animals respiring proteins and carbohydrates. In addition, the lipid-rich copepods, thought to be exiting diapause, had low specific ingestion rates which can be at least partially attributed to these animals being somewhat reliant upon the consumption of stored lipids.

The prevalence of lipid storing copepods substantially complicates mesopelagic carbon budgeting. Stored lipids represent carbon ingested during the previous growing season, meaning lipids are integrating over very different time scales to those that are observed in the observational field programme (e.g. vertical patterns of flux attenuation)..

CRediT author statement

KC conceptualised the manuscript with support from all authors. AB, DM, GS, KC, GS, GT and SF conducted on board sample collection and processing. AB, DBJ, KC, ME and SB conducted laboratory analysis of samples. GW and RS provided supporting data and technical expertise. All authors contributed to the writing of the manuscript.

Acknowledgements

The authors are grateful to the crew of the R.R.S. Discovery and participants of cruise DY086 for help collecting samples. We are indebted to May Gomez, Ted Packard and Ico Martinez (EOMAR), Santiago Hernández León, Laia Armengol, and Ione Medina Suarez (IOCAG) for training in ETS assay methods and to Brian Dickie (University of Southampton) for the emergency provision of a

spectrophotometer. The authors also wish to thank the three anonymous reviewers whose comments have greatly improved this manuscript. This work was supported by the NERC funded Large Grant, COMICS (NE/M020762/1; NE/M020835/1).

References

Ainsworth, J., Poulton, A. J., Lohan, M. C., Stinchcombe, M. C., Lough, A. J. M., and Moore, C. M. 2023. Iron cycling during the decline of a South Georgia diatom bloom. Deep Sea Research Part II: Topical Studies in Oceanography, 208: 105269. DOI 10.1016/j.dsr2.2023.105269

Alldredge, A. 1998. The carbon, nitrogen and mass content of marine snow as a function of aggregate size. Deep Sea Research Part I: Oceanographic Research Papers, 45: 529-541. DOI 10.1016/S0967-0637(97)00048-4

Anderson, T. R., Pond, D. W., and Mayor, D. J. 2017. The role of microbes in the nutrition of detritivorous invertebrates: A stoichiometric analysis. Frontiers in Microbiology, 7. DOI 10.3389/fmicb.2016.02113

Andrews, K. J. H. 1966. The distribution and life history of *Calanoides acutus* (Giesbrecht). Discovery Reports, 34: 117-162.

Archibald, K. M., Siegel, D. A., and Doney, S. C. 2019. Modeling the impact of zooplankton diel vertical migration on the carbon export flux of the biological pump. Global Biogeochemical Cycles, 33: 181-199. DOI 10.1029/2018GB005983

Ariza, A., Garijo, J. C., Landeira, J. M., Bordes, F., and Hernández-León, S. 2015. Migrant biomass and respiratory carbon flux by zooplankton and micronekton in the subtropical northeast Atlantic Ocean (Canary Islands). Progress in Oceanography, 134: 330-342. DOI 10.1016/j.pocean.2015.03.003

Atkinson, A. 1995. Omnivory and feeding selectivity in five copepod species during spring in the Bellingshausen Sea, Antarctica. ICES Journal of Marine Science, 52: 385-396. DOI 10.1016/1054-3139(95)80054-9

Atkinson, A. 1996. Subantarctic copepods in an oceanic, low chlorophyll environment: ciliate predation, food selectivity and impact on prey populations. Marine Ecology Progress Series, 130: 85-96. DOI 10.3354/meps130085

Atkinson, A., Shreeve, R. S., Pakhomov, E. A., Priddle, J., Blight, S. P., and Ward, P. 1996. Zooplankton response to a phytoplankton bloom near South Georgia, Antarctica. Marine Ecology Progress Series, 144: 195-210. DOI 10.3354/meps144195

Atkinson, A., Ward, P., Hunt, B. P. V., Pakhomov, E. A., and Hosie, G. W. 2012. An overview of Southern Ocean zooplankton data: abundance, biomass, feeding and functional relationships. CCAMLR Science, 19: 171-218.

Atkinson, A., Ward, P., Williams, R., and Poulet, S. A. 1992. Feeding rates and diel vertical migration of copepods near South Georgia: comparison of shelf and oceanic sites. Marine Biology, 114: 49-56. DOI 10.1007/BF00350855

Baker, A. d. C., Clarke, M. R., and Harris, M. J. 1973. The N.I.O. combination net (RMT 1 + 8) and further developments of rectangular midwater trawls. Journal of the Marine Biological Association of the United Kingdom, 53: 167-184. DOI 10.1017/S0025315400056708

Bandara, K., Varpe, Ø., Wijewardene, L., Tverberg, V., and Eiane, K. 2021. Two hundred years of zooplankton vertical migration research. Biological Reviews, 96: 1547-1589. DOI 10.1111/brv.12715

Belcher, A., Cook, K., Bondyale-Juez, D., Stowasser, G., Fielding, S., Saunders, R. A., Mayor, D. J., et al. 2020. Respiration of mesopelagic fish: a comparison of respiratory electron transport system

(ETS) measurements and allometrically calculated rates in the Southern Ocean and Benguela Current. ICES Journal of Marine Science, 77: 1672–1684. DOI 10.1093/icesjms/fsaa031

Belcher, A., Henson, S. A., Manno, C., Hill, S. L., Atkinson, A., Thorpe, S. E., Fretwell, P., et al. 2019a. Krill faecal pellets drive hidden pulses of particulate organic carbon in the marginal ice zone. Nature Communications, 10: 889. DOI 10.1038/s41467-019-08847-1

Belcher, A., Iversen, M., Manno, C., Henson, S. A., Tarling, G. A., and Sanders, R. 2016. The role of particle associated microbes in remineralization of fecal pellets in the upper mesopelagic of the Scotia Sea, Antarctica. Limnology and Oceanography, 61: 1049-1064. DOI 10.1002/lno.10269

Belcher, A., Saunders, R. A., and Tarling, G. A. 2019b. Respiration rates and active carbon flux of mesopelagic fishes (Family Myctophidae) in the Scotia Sea, Southern Ocean. Marine Ecology Progress Series, 610: 149-162. DOI 10.3354/meps12861

Bernard, K. S., and Froneman, P. W. 2003. Mesozooplankton community structure and grazing impact in the Polar Frontal Zone of the south Indian Ocean during austral autumn 2002. Polar Biology, 26: 268-275. DOI 10.1007/s00300-002-0472-x

Bondyale-Juez, D. R., Packard, T. T., Viera-Rodríguez, M. A., and Gómez, M. 2017. Respiration: comparison of the Winkler technique, O_2 electrodes, O_2 optodes and the respiratory electron transport system assay. Marine Biology, 164: 226. DOI 10.1007/s00227-017-3271-1

Boyd, P. W., Claustre, H., Levy, M., Siegel, D. A., and Weber, T. 2019. Multi-faceted particle pumps drive carbon sequestration in the ocean. Nature, 568: 327-335. DOI 10.1038/s41586-019-1098-2

Briggs, N., Dall'Olmo, G., and Claustre, H. 2020. Major role of particle fragmentation in regulating biological sequestration of CO_2 by the oceans. Science, 367: 791-793. DOI 10.1126/science.aay1790

Buesseler, K. O., Lamborg, C. H., Boyd, P. W., Lam, P. J., Trull, T. W., Bidigare, R. R., Bishop, J. K. B., et al. 2007. Revisiting carbon flux through the ocean's twilight zone. Science, 316: 567-570. DOI 10.1126/science.1137959

Burd, A. B., Hansell, D. A., Steinberg, D. K., Anderson, T. R., Arístegui, J., Baltar, F., Beaupré, S. R., et al. 2010. Assessing the apparent imbalance between geochemical and biochemical indicators of meso- and bathypelagic biological activity: What the @$♯! is wrong with present calculations of carbon budgets? Deep-Sea Research Part II: Topical Studies in Oceanography, 57: 1557-1571. DOI 10.1016/j.dsr2.2010.02.022

Cisewski, B., and Strass, V. H. 2016. Acoustic insights into the zooplankton dynamics of the eastern Weddell Sea. Progress in Oceanography, 144: 62-92. DOI 10.1016/j.pocean.2016.03.005

Cisewski, B., Strass, V. H., Rhein, M., and Krägefsky, S. 2010. Seasonal variation of diel vertical migration of zooplankton from ADCP backscatter time series data in the Lazarev Sea, Antarctica. Deep Sea Research Part I: Oceanographic Research Papers, 57: 78-94. DOI 10.1016/j.dsr.2009.10.005

Collins, M. A., Stowasser, G., Fielding, S., Shreeve, R., Xavier, J. C., Venables, H. J., Enderlein, P., et al. 2012. Latitudinal and bathymetric patterns in the distribution and abundance of mesopelagic fish in the Scotia Sea. Deep Sea Research Part II: Topical Studies in Oceanography, 59-60: 189-198. DOI 10.1016/j.dsr2.2011.07.003

Conroy, J. A., Steinberg, D. K., Thibodeau, P. S., and Schofield, O. 2020. Zooplankton diel vertical migration during Antarctic summer. Deep Sea Research Part I: Oceanographic Research Papers, 162: 103324. DOI 10.1016/j.dsr.2020.103324

Cotté, C., Ariza, A., Berne, A., Habasque, J., Lebourges-Dhaussy, A., Roudaut, G., Espinasse, B., et al. 2022. Macrozooplankton and micronekton diversity and associated carbon vertical patterns and fluxes under distinct productive conditions around the Kerguelen Islands. Journal of Marine Systems, 226: 103650. DOI 10.1016/j.jmarsys.2021.103650

De Robertis, A. 2002. Size-dependent visual predation risk and the timing of vertical migration: An optimization model. Limnology and Oceanography, 47: 925-933. DOI 10.4319/lo.2002.47.4.0925

Demer, D. A., Berger, L., Bernasconi, M., Bethke, E., Boswell, K., Chu, D., Domokos, R., et al. 2015. Calibration of acoustic instruments. 326. 133pp. pp.

Drits, A. V., Pasternak, A. F., and Kosobokova, K. N. 1994. Physiological characteristics of the antarctic copepod *Calanoides acutus* during late summer in the Weddell Sea. Hydrobiologia, 292: 201-207. DOI 10.1007/BF00229942

Flores, H., Hunt, B. P. V., Kruse, S., Pakhomov, E. A., Siegel, V., van Franeker, J. A., Strass, V., et al. 2014. Seasonal changes in the vertical distribution and community structure of Antarctic macrozooplankton and micronekton. Deep Sea Research Part I: Oceanographic Research Papers, 84: 127-141. DOI 10.1016/j.dsr.2013.11.001

Forward, R. B., Jr. 1988. Diel vertical migration: zooplankton photobiology and behaviour. Oceanography and Marine Biology: An Annual Review, 26: 361-393.

Francois, R. E., and Garrison, G. R. 1982. Sound absorption based on ocean measurements. Part II: Boric acid contribution and equation for total absorption. The Journal of the Acoustical Society of America, 72: 1879-1890. DOI 10.1121/1.388673

Frost, B. W. 1972. Effects of size and concentration of food particles on the feeding behaviour of the marine planktonic copepods *Calanus pacificus*. Limnology and Oceanography, 17: 805-815. DOI 10.4319/lo.1972.17.6.0805

Giering, S., Ainsworth, J., Ashurst, D., Belcher, A., Bridger, M., Carvalho, F., Cook, K., et al. 2019a. RRS Discovery Cruise DY086, 12 November – 19 December 2017. Controls over Ocean Mesopelagic Carbon Storage (COMICS). No. 55. 265pp. pp.

Giering, S. L. C., Sanders, R., Blackbird, S., Briggs, N., Carvalho, F., East, H., Espinola, B., et al. 2023. Vertical imbalance in organic carbon budgets is indicative of a missing vertical transfer during a phytoplankton bloom near South Georgia (COMICS). Deep Sea Research Part II: Topical Studies in Oceanography, 209: 105277. DOI 10.1016/j.dsr2.2023.105277

Giering, S. L. C., Sanders, R., Lampitt, R. S., Anderson, T. R., Tamburini, C., Boutrif, M., Zubkov, M. V., et al. 2014. Reconciliation of the carbon budget in the ocean's twilight zone. Nature, 507: 480-483. DOI 10.1038/nature13123

Giering, S. L. C., Wells, S. R., Mayers, K. M. J., Schuster, H., Cornwell, L., Fileman, E., Atkinson, A., et al. 2019b. Seasonal variation of zooplankton community structure and trophic position in the Celtic Sea: a stable isotope and biovolume spectrum approach. Progress in Oceanography, 177: 101943. DOI 10.1016/j.pocean.2018.03.012

Gómez, M., Torres, S., and Hernández-León, S. 1996. Modification of the electron transport system (ETS) method for routine measurements of respiratory rates of zooplankton. South African Journal of Marine Science, 17: 15-20. DOI 10.2989/025776196784158446

Hansen, A. N., and Visser, A. W. 2016. Carbon export by vertically migrating zooplankton: an optimal behavior model. Limnology and Oceanography, 61: 701-710. DOI 10.1002/lno.10249

Hernández-León, S., Almeida, C., Portillo-Hahnefeld, A., Gómez, M., and Montero, I. 2000. Biomass and potential feeding, respiration and growth of zooplankton in the Bransfield Strait (Antarctic Peninsula) during austral summer. Polar Biology, 23: 679-690. DOI 10.1007/s003000000139

Hernández-León, S., Calles, S., and Fernández de Puelles, M. L. 2019a. The estimation of metabolism in the mesopelagic zone: Disentangling deep-sea zooplankton respiration. Progress in Oceanography, 178: 102163. DOI 10.1016/j.pocean.2019.102163

Hernández-León, S., and Gómez, M. 1996. Factors affecting the respiration/ETS ratio in marine zooplankton. Journal of Plankton Research, 18: 239-255. DOI 10.1093/plankt/18.2.239

Hernández-León, S., and Ikeda, T. 2005. Zooplankton respiration. *In* Respiration in Aquatic Ecosystems. Ed. by P. A. d. Giorgio, and P. J. l. Williams. Oxford University Press.

Hernández-León, S., Olivar, M. P., Fernández de Puelles, M. L., Bode, A., Castellón, A., López-Pérez, C., Tuset, V. M., et al. 2019b. Zooplankton and micronekton active flux across the tropical and subtropical Atlantic Ocean. Frontiers in Marine Science, 6. DOI 10.3389/fmars.2019.00535

Hernández-León, S., Putzeys, S., Almeida, C., Bécognée, P., Marrero-Díaz, A., Arístegui, J., and Yebra, L. 2019c. Carbon export through zooplankton active flux in the Canary Current. Journal of Marine Systems, 189: 12-21. DOI 10.1016/j.jmarsys.2018.09.002

Hidaka, K., Kawaguchi, K., Murakami, M., and Takahashi, M. 2001. Downward transport of organic carbon by diel migratory micronekton in the western equatorial Pacific:: its quantitative and qualitative importance. Deep Sea Research Part I: Oceanographic Research Papers, 48: 1923-1939. DOI 10.1016/S0967-0637(01)00003-6

Hirche, H.-J. 1984. Temperature and metabolism of plankton—I. Respiration of antarctic zooplankton at different temperatures with a comparison of antarctic and nordic krill. Comparative Biochemistry and Physiology Part A: Physiology, 77: 361-368. DOI 10.1016/0300-9629(84)90074-4

Ikeda, T. 1985. Metabolic rates of epipelagic marine zooplankton as a function of body mass and temperature. Marine Biology, 85: 1-11. DOI 10.1007/bf00396409

Ikeda, T. 2014. Respiration and ammonia excretion by marine metazooplankton taxa: synthesis toward a global-bathymetric model. Marine Biology, 161: 2753-2766. DOI 10.1007/s00227-014-2540-5

Ikeda, T. 2016. Routine metabolic rates of pelagic marine fishes and cephalopods as a function of body mass, habitat temperature and habitat depth. Journal of Experimental Marine Biology and Ecology, 480: 74-86. DOI 10.1016/j.jembe.2016.03.012

Ikeda, T., Sano, F., Yamaguchi, A., and Matsuishi, T. 2006. Metabolism of mesopelagic and bathypelagic copepods in the western North Pacific Ocean. Marine Ecology Progress Series, 322: 199-211. DOI 10.3354/meps322199

Kaartvedt, S., Staby, A., and Aksnes, D. L. 2012. Efficient trawl avoidance by mesopelagic fishes causes large underestimation of their biomass. Marine Ecology Progress Series, 456: 1-6. DOI 10.3354/meps09785

Kelly, T. B., Davison, P. C., Goericke, R., Landry, M. R., Ohman, M. D., and Stukel, M. R. 2019. The importance of mesozooplankton diel vertical migration for sustaining a mesopelagic food web. Frontiers in Marine Science, 6. DOI 10.3389/fmars.2019.00508

Kiørboe, T. 2013. Zooplankton body composition. Limnology and Oceanography, 58: 1843-1850. DOI 10.4319/lo.2013.58.5.1843

Kiørboe, T., and Hirst, A. G. 2014. Shifts in mass scaling of respiration, feeding, and growth rates across life-form transitions in marine pelagic organisms. The American Naturalist, 183: E118-E130. DOI 10.1086/675241

Kittel, W., Witek, Z., and Czykieta, H. 1985. Distribution of *Euphausia frigida*, *Euphausia crystallorophias*, *Euphausia triacantha* and *Thysanoessa macrura* in the southern part of Drake Passage and in the Bransfield Strait during the 1983—1984 austral summer (BIOMASS-SIBEX). Polish Polar Research, 6: 133-149.

Korb, R. E., Whitehouse, M. J., Ward, P., Gordon, M., Venables, H. J., and Poulton, A. J. 2012. Regional and seasonal differences in microplankton biomass, productivity, and structure across the Scotia Sea: Implications for the export of biogenic carbon. Deep Sea Research Part II: Topical Studies in Oceanography, 59-60: 67-77. DOI 10.1016/j.dsr2.2011.06.006

Koski, M., Boutorh, J., and de la Rocha, C. 2017. Feeding on dispersed vs. aggregated particles: The effect of zooplankton feeding behavior on vertical flux. PLoS ONE, 12: e0177958. DOI 10.1371/journal.pone.0177958

Koski, M., Valencia, B., Newstead, R., and Thiele, C. 2020. The missing piece of the upper mesopelagic carbon budget? Biomass, vertical distribution and feeding of aggregate-

associated copepods at the PAP site. Progress in Oceanography, 181: 102243. DOI 10.1016/j.pocean.2019.102243
Kwon, E. Y., Primeau, F., and Sarmiento, J. L. 2009. The impact of remineralization depth on the air–sea carbon balance. Nature Geoscience, 2: 630-635. DOI 10.1038/ngeo612
Kwong, L. E., Henschke, N., Pakhomov, E. A., Everett, J. D., and Suthers, I. M. 2020. Mesozooplankton and micronekton active carbon transport in contrasting eddies. Frontiers in Marine Science, 6. DOI 10.3389/fmars.2019.00825
Landry, M. R., Stukel, M. R., and Décima, M. 2020. Food-web fluxes support high rates of mesozooplankton respiration and production in the equatorial Pacific. Marine Ecology Progress Series, 652: 15-32. DOI 10.3354/meps13479
Le Moigne, F. A. C. 2019. Pathways of organic carbon downward transport by the oceanic biological carbon pump. Frontiers in Marine Science, 6. DOI 10.3389/fmars.2019.00634
Liszka, C. M., Manno, C., Stowasser, G., Robinson, C., and Tarling, G. A. 2019. Mesozooplankton community composition controls fecal pellet flux and remineralization depth in the Southern Ocean. Frontiers in Marine Science, 6. DOI 10.3389/fmars.2019.00230
Longhurst, A. R., Bedo, A. W., Harrison, W. G., Head, E. J. H., and Sameoto, D. D. 1990. Vertical flux of respiratory carbon by oceanic diel migrant biota. Deep Sea Research Part A. Oceanographic Research Papers, 37: 685-694. DOI 10.1016/0198-0149(90)90098-G
Maas, A. E., Miccoli, A., Stamieszkin, K., Carlson, C. A., and Steinberg, D. K. 2021. Allometry and the calculation of zooplankton metabolism in the subarctic Northeast Pacific Ocean. Journal of Plankton Research, 43: 413-427. DOI 10.1093/plankt/fbab026
Mackenzie, K. V. 1981. Nine-term equation for sound speed in the oceans. The Journal of the Acoustical Society of America, 70: 807-812. DOI 10.1121/1.386920
Maldonado, F., Packard, T. T., and Gómez, M. 2012. Understanding tetrazolium reduction and the importance of substrates in measuring respiratory electron transport activity. Journal of Experimental Marine Biology and Ecology, 434-435: 110-118. DOI 10.1016/j.jembe.2012.08.010
Manno, C., Stowasser, G., Enderlein, P., Fielding, S., and Tarling, G. A. 2015. The contribution of zooplankton faecal pellets to deep-carbon transport in the Scotia Sea (Southern Ocean). Biogeosciences, 12: 1955-1965. DOI 10.5194/bg-12-1955-2015
Manno, C., Stowasser, G., Fielding, S., Apeland, B., and Tarling, G. A. 2022. Deep carbon export peaks are driven by different biological pathways during the extended Scotia Sea (Southern Ocean) bloom. Deep Sea Research (Part II, Topical Studies in Oceanography), 205. DOI 10.1016/j.dsr2.2022.105183
Mayor, D. J., Anderson, T. R., Irigoien, X., and Harris, R. 2006. Feeding and reproduction of *Calanus finmarchicus* during non-bloom conditions in the Irminger Sea. Journal of Plankton Research, 28: 1167-1179. DOI 10.1093/plankt/fbl047
Mayor, D. J., Cook, K., Thornton, B., Walsham, P., Witte, U. F. M., Zuur, A. F., and Anderson, T. R. 2011. Absorption efficiencies and basal turnover of C, N and fatty acids in a marine Calanoid copepod. Functional Ecology, 25: 509-518. DOI 10.1111/j.1365-2435.2010.01791.x
Mayor, D. J., Gentleman, W. C., and Anderson, T. R. 2020. Ocean carbon sequestration: Particle fragmentation by copepods as a significant unrecognised factor? Bioessays, 42: 2000149. DOI 10.1002/bies.202000149
Mayor, D. J., Sanders, R., Giering, S. L. C., and Anderson, T. R. 2014. Microbial gardening in the ocean's twilight zone: Detritivorous metazoans benefit from fragmenting, rather than ingesting, sinking detritus. Bioessays: n/a-n/a. DOI 10.1002/bies.201400100
Mayzaud, P., Razouls, S., Errhif, A., Tirelli, V., and Labat, J. P. 2002a. Feeding, respiration and egg production rates of copepods during austral spring in the Indian sector of the Antarctic Ocean: role of the zooplankton community in carbon transformation. Deep Sea Research Part I: Oceanographic Research Papers, 49: 1027-1048. DOI 10.1016/S0967-0637(02)00012-2

Mayzaud, P., Tirelli, V., Errhif, A., Labat, J. P., Razouls, S., and Perissinotto, R. 2002b. Carbon intake by zooplankton. Importance and role of zooplankton grazing in the Indian sector of the Southern Ocean. Deep Sea Research Part II: Topical Studies in Oceanography, 49: 3169-3187. DOI 10.1016/S0967-0645(02)00077-2

Menden-Deuer, S., and Lessard, E. J. 2000. Carbon to volume relationships for dinoflagellates, diatoms, and other protist plankton. Limnology and Oceanography, 45: 569-579. DOI 10.4319/lo.2000.45.3.0569

Omand, M. M., Steinberg, D. K., and Stamieszkin, K. 2021. Cloud shadows drive vertical migrations of deep-dwelling marine life. Proceedings of the National Academy of Sciences, 118: e2022977118. DOI 10.1073/pnas.2022977118

Osma, N., Fernández-Urruzola, I., Gómez, M., Montesdeoca-Esponda, S., and Packard, T. T. 2016a. Predicting in vivo oxygen consumption rate from ETS activity and bisubstrate enzyme kinetics in cultured marine zooplankton. Marine Biology, 163: 146. DOI 10.1007/s00227-016-2923-x

Osma, N., Maldonado, F., Fernández-Urruzola, I., Packard, T. T., and Gómez, M. 2016b. Variability of respiration and pyridine nucleotides concentration in oceanic zooplankton. Journal of Plankton Research, 38: 537-550. DOI 10.1093/plankt/fbw001

Owens, T. G., and King, F. D. 1975. The measurement of respiratory electron-transport-system activity in marine zooplankton. Marine Biology, 30: 27-36. DOI 10.1007/BF00393750

Packard, T. T., and Christensen, J. P. 2004. Respiration and vertical carbon flux in the Gulf of Maine water column. Journal of Marine Research, 62: 93-115. DOI 10.1357/00222400460744636

Packard, T. T., Devol, A. H., and King, F. D. 1975. The effect of temperature on the respiratory electron transport system in marine plankton. Deep Sea Research and Oceanographic Abstracts, 22: 237-249. DOI 10.1016/0011-7471(75)90029-7

Pakhomov, E. A., Froneman, P. W., Wassmann, P., Ratkova, T., and Arashkevich, E. 2002. Contribution of algal sinking and zooplankton grazing to downward flux in the Lazarev Sea (Southern Ocean) during the onset of phytoplankton bloom: a lagrangian study. Marine Ecology Progress Series, 233: 73-88. DOI 10.3354/meps233073

Pakhomov, E. A., Perissinotto, R., and McQuaid, C. D. 1996. Prey composition and daily rations of myctophid fishes in the Southern Ocean. Marine Ecology Progress Series, 134: 1-14. DOI 10.3354/meps134001

Piatkowski, U., Rodhouse, P. G., White, M. G., Bone, D. G., and Symon, C. 1994. Nekton community of the Scotia Sea as sampled by the RMT 25 during austral summer. Marine Ecology Progress Series, 112: 13-28. DOI 10.3354/meps112013

Platnick, S., Hubanks, P., Meyer, K., and King, M. D. 2015. MODIS Atmosphere L3 Monthly Product (08_L3). NASA MODIS Adaptive Processing System, Goddard Space Flight Center.

Polimene, L., Sailley, S., Clark, D., Mitra, A., and Allen, J. I. 2017. Biological or microbial carbon pump? The role of phytoplankton stoichiometry in ocean carbon sequestration. Journal of Plankton Research, 39: 180-186. DOI 10.1093/plankt/fbw091

Prosser, C. L. 1961. Oxygen: respiration and metabolism. *In* Comparative Animal Physiology, pp. 165-211. Ed. by C. L. Prosser, and J. F.A. Brown. W.B. Saunders, Philadelphia.

Razouls, S., Du Réau, G., Guillot, P., Maison, J., and Jeandel, C. 1998. Seasonal abundance of copepod assemblages and grazing pressure in the Kerguelen Island area (Southern Ocean). Journal of Plankton Research, 20: 1599-1614. DOI 10.1093/plankt/20.8.1599

Riley, J. S., Sanders, R., Marsay, C., Le Moigne, F. A. C., Achterberg, E. P., and Poulton, A. J. 2012. The relative contribution of fast and slow sinking particles to ocean carbon export. Global Biogeochemical Cycles, 26: GB1026. DOI 10.1029/2011GB004085

Sanders, R. J., Henson, S. A., Martin, A. P., Anderson, T. R., Bernardello, R., Enderlein, P., Fielding, S., et al. 2016. Controls over Ocean Mesopelagic Interior Carbon Storage (COMICS): Fieldwork, synthesis, and modeling efforts. Frontiers in Marine Science, 3. DOI 10.3389/fmars.2016.00136

1062 Sarthou, G., Vincent, D., Christaki, U., Obernosterer, I., Timmermans, K. R., and Brussaard, C. P. D.
1063 2008. The fate of biogenic iron during a phytoplankton bloom induced by natural
1064 fertilisation: Impact of copepod grazing. Deep Sea Research Part II: Topical Studies in
1065 Oceanography, 55: 734-751. DOI 10.1016/j.dsr2.2007.12.033
1066 Siegel, V. 1987. Age and growth of Antarctic Euphausiacea (Crustacea) under natural conditions.
1067 Marine Biology, 96: 483-495. DOI 10.1007/BF00397966
1068 Siegel, V. 1992. Review of length-weight relationships for Antarctic Krill. SC-CAMLR Selected
1069 Scientific Papers, 9: 145-155.
1070 Steinberg, D. K., Carlson, C. A., Bates, N. R., Goldthwait, S. A., Madin, L. P., and Michaels, A. F. 2000.
1071 Zooplankton vertical migration and the active transport of dissolved organic and inorganic
1072 carbon in the Sargasso Sea. Deep Sea Research Part I: Oceanographic Research Papers, 47:
1073 137-158. DOI 10.1016/S0967-0637(99)00052-7
1074 Steinberg, D. K., and Landry, M. R. 2017. Zooplankton and the Ocean Carbon Cycle. Annual Review of
1075 Marine Science, 9: 413-444. DOI 10.1146/annurev-marine-010814-015924
1076 Steinberg, D. K., Van Mooy, B. A. S., Buesseler, K. O., Boyd, P. W., Kobari, T., and Karl, D. M. 2008.
1077 Bacterial vs. zooplankton control of sinking particle flux in the ocean's twilight zone.
1078 Limnology and Oceanography, 53: 1327-1338. DOI 10.4319/lo.2008.53.4.1327
1079 Swadling, K. M., Gibson, J. A. E., Ritz, D. A., Nichols, P. D., and Hughes, D. E. 1997. Grazing of
1080 phytoplankton by copepods in eastern Antarctic coastal waters. Marine Biology, 128: 39-48.
1081 DOI 10.1007/s002270050066
1082 Tarling, G. A., and Johnson, M. L. 2006. Satiation gives krill that sinking feeling. Current Biology, 16:
1083 R83-R84. DOI 10.1016/j.cub.2006.01.044
1084 Tarling, G. A., and Thorpe, S. E. 2017. Oceanic swarms of Antarctic krill perform satiation sinking.
1085 Proceedings of the Royal Society B: Biological Sciences, 284: 20172015. DOI
1086 10.1098/rspb.2017.2015
1087 Tarling, G. A., Ward, P., Atkinson, A., Collins, M. A., and Murphy, E. J. 2012. DISCOVERY 2010: Spatial
1088 and temporal variability in a dynamic polar ecosystem. Deep Sea Research Part II: Topical
1089 Studies in Oceanography, 59-60: 1-13. DOI 10.1016/j.dsr2.2011.10.001
1090 Turner, J. T. 2015. Zooplankton fecal pellets, marine snow, phytodetritus and the ocean's biological
1091 pump. Progress in Oceanography, 130: 205-248. DOI 10.1016/j.pocean.2014.08.005
1092 Ward, P., Atkinson, A., and Tarling, G. 2012. Mesozooplankton community structure and variability in
1093 the Scotia Sea: A seasonal comparison. Deep Sea Research Part II: Topical Studies in
1094 Oceanography, 59-60: 78-92. DOI 10.1016/j.dsr2.2011.07.004
1095 Wiebe, P. H., and Benfield, M. C. 2003. From the Hensen net toward four-dimensional biological
1096 oceanography. Progress in Oceanography, 56: 7-136. DOI 10.1016/S0079-6611(02)00140-4
1097 Yang, G., Han, Z., Pan, J., Zhou, K., Wang, Y., and Li, C. 2019. Contribution of zooplankton faecal
1098 pellets to carbon transport of the mesopelagic layers in the polynya region of Prydz Bay,
1099 Antarctica. Estuarine, Coastal and Shelf Science, 222: 139-146. DOI
1100 10.1016/j.ecss.2019.04.006
1101 Yebra, L., Herrera, I., Mercado, J. M., Cortés, D., Gómez-Jakobsen, F., Alonso, A., Sánchez, A., et al.
1102 2018. Zooplankton production and carbon export flux in the western Alboran Sea gyre (SW
1103 Mediterranean). Progress in Oceanography, 167: 64-77. DOI 10.1016/j.pocean.2018.07.009
1104 Zøllner, E., Hoppe, H. G., Sommer, U., and Jürgens, K. 2009. Effect of zooplankton-mediated trophic
1105 cascades on marine microbial food web components (bacteria, nanoflagellates, ciliates).
1106 Limnology and Oceanography, 54: 262-275. DOI 10.4319/lo.2009.54.1.0262

1107

Figure captions

Figure 1: Dominant taxa (by % of total carbon biomass) of mesozooplankton (Bongo net >100 µm; MOCNESS >330 µm) and micronekton (>4mm RMT25) biomass at station P3 (A-C) in the Scotia Sea (day and night combined). The 'Euphausiacea' category consisted of all species except *Euphausia superba* in the MOCNESS samples, and all species including *E. superba* in the RMT samples. The 'Other' category consisted of gastropods, ostracods, appendicularians and decapod larvae in the Bongo net samples; amphipods, appendicularians, chaetognaths, ostracods, polychaetes, pteropods, salps and siphonophores in the MOCNESS samples; and amphipods, cephalopods, chaetognaths, decapods, ostracods, polychaetes, and pteropods in the RMT samples.

Figure 2: Carbon biomass (mmolC m^{-3}) of mesozooplankton (Bongo net >100 µm; MOCNESS >330 µm) and micronekton (>4mm RMT25) at station P3 (A-C) in the Scotia Sea. Note the different scales on the x-axes. MOCNESS biomass samples were not collected during P3A.

Figure 3: Difference in day and night Weighted Mean Depth (∆WMD, m) of dominant taxa collected by the MOCNESS (>330 µm) and RMT25 net (> 4 mm) during stations P3A, P3B and P3C. Negative values indicate deeper WMD during the day. MOCNESS biomass samples were not collected during P3A.

Figure 4: Total community respiration (mmolC m^{-3} d^{-1}) of mesozooplankton (Bongo net >100 µm; MOCNESS >330 µm) and micronekton (>4mm RMT25) at station P3 (A-C) in the Scotia Sea. Note the different scales on the x-axes.

Figure 5: Total community ingestion (mmolC m^{-3} d^{-1}) of mesozooplankton (Bongo net >100 µm; MOCNESS >330 µm) and micronekton (>4mm RMT25) at station P3 (A-C) in the Scotia Sea. Note the different scales on the x-axes.

Figure 6: Total pelagic community ingestion and respiration (mmolC m^{-3} d^{-1}) at station P3 in the Scotia Sea. P3B-D-N = station P3B deep night, P3B-D-D = station P3B deep day, P3B-S-N = station P3B shallow night, P3B-S-D = station P3B shallow day, P3C-D-N = station P3C deep night, P3C-D-D = station P3C deep day, P3C-S-N = station P3C shallow night, P3C-S-D = station P3C shallow day. Deep= 250-500m, shallow = 0-250m.

1140

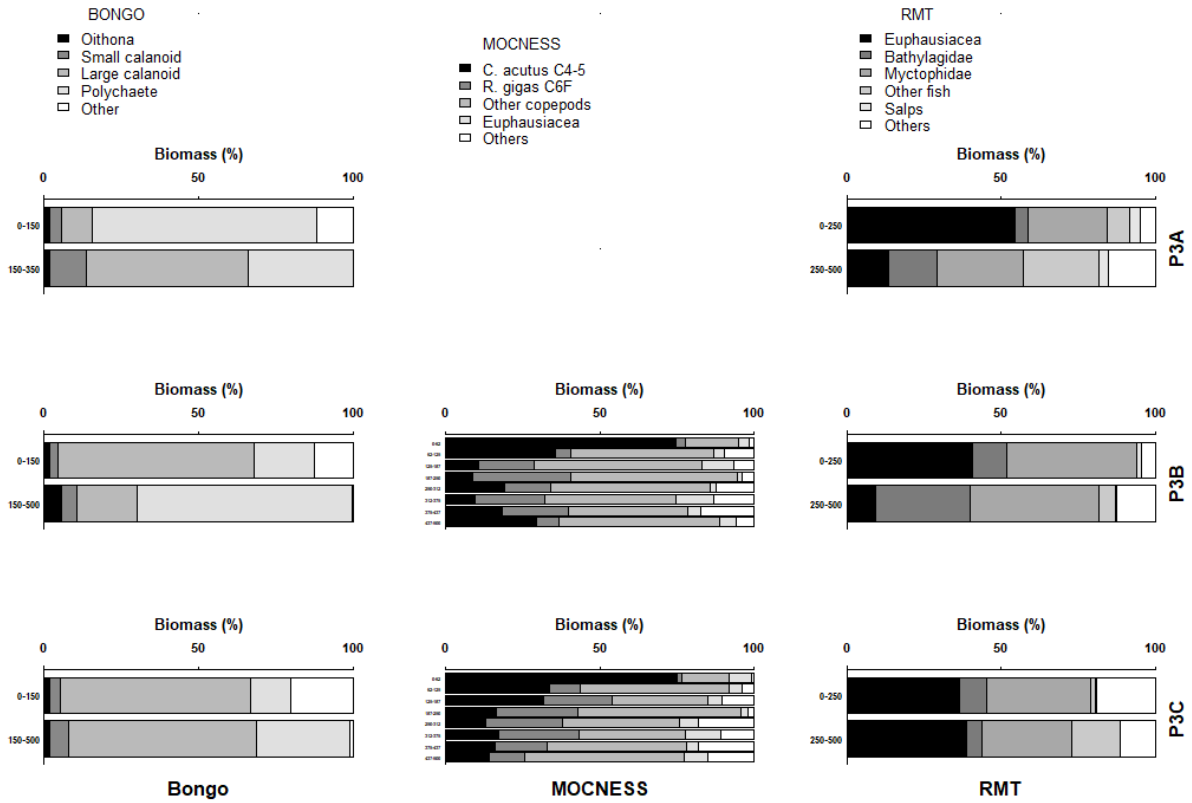

1141

1142

1143 **Figure 1**

1144

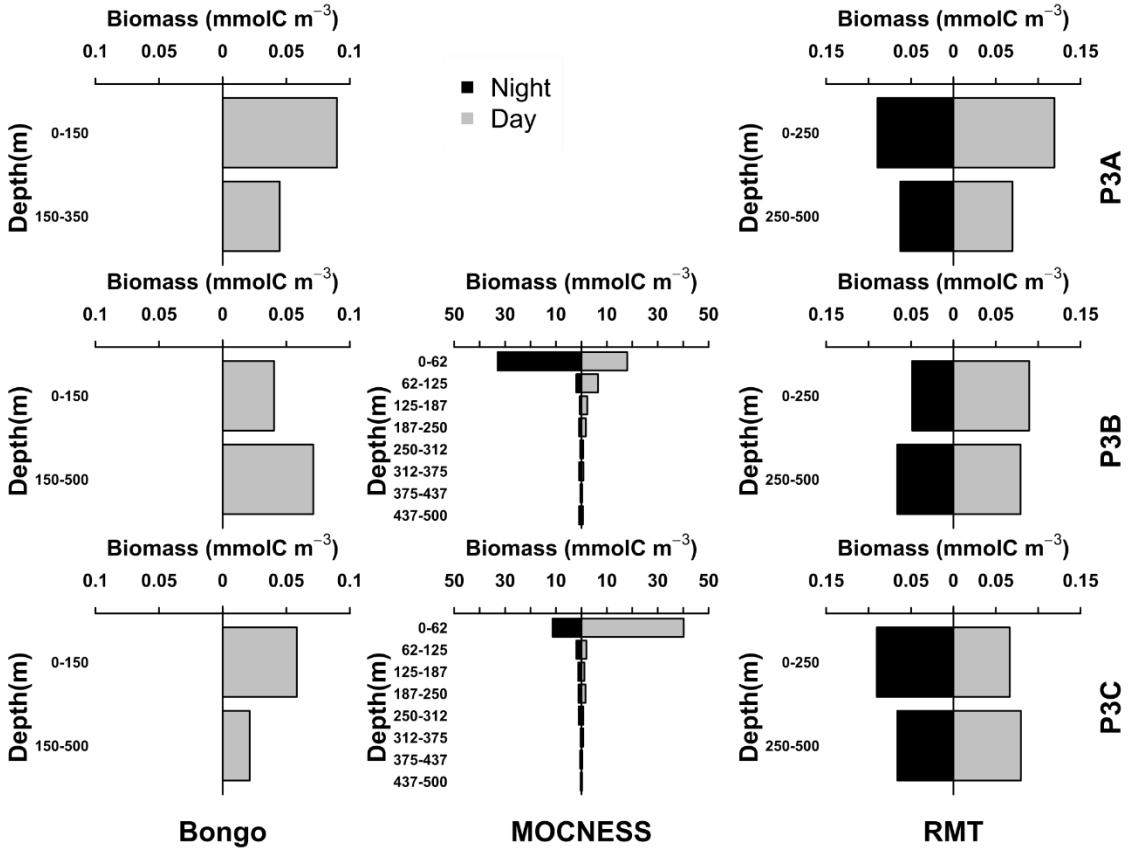

1145

1146 **Figure 2**

1147

1148

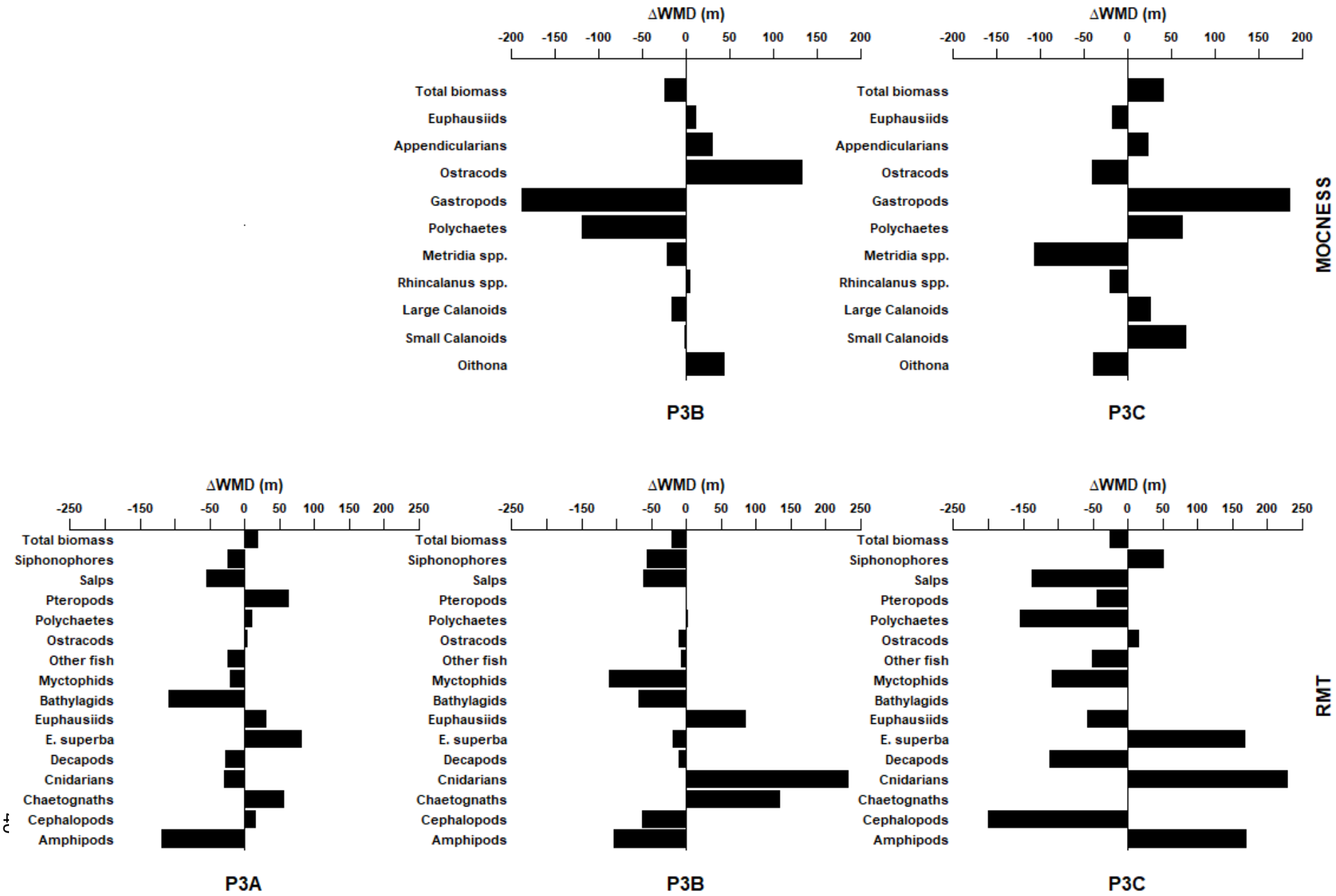
ΔWMD (m)
-200 -150 -100 -50 0 50 100 150 200
Total biomass
Euphausiids
Appendicularians
Ostracods
Gastropods
Polychaetes
Metridia spp.
Rhincalanus spp.
Large Calanoids
Small Calanoids
Oithona
P3B
P3C
MOCNESS
ΔWMD (m)
-250 -150 -50 0 50 100 150 200 250
Total biomass
Siphonophores
Salps
Pteropods
Polychaetes
Ostracods
Other fish
Myctophids
Bathylagids
Euphausiids
E. superba
Decapods
Cnidarians
Chaetognaths
Cephalopods
Amphipods
P3A
P3B
P3C
RMT

Figure 3

1152

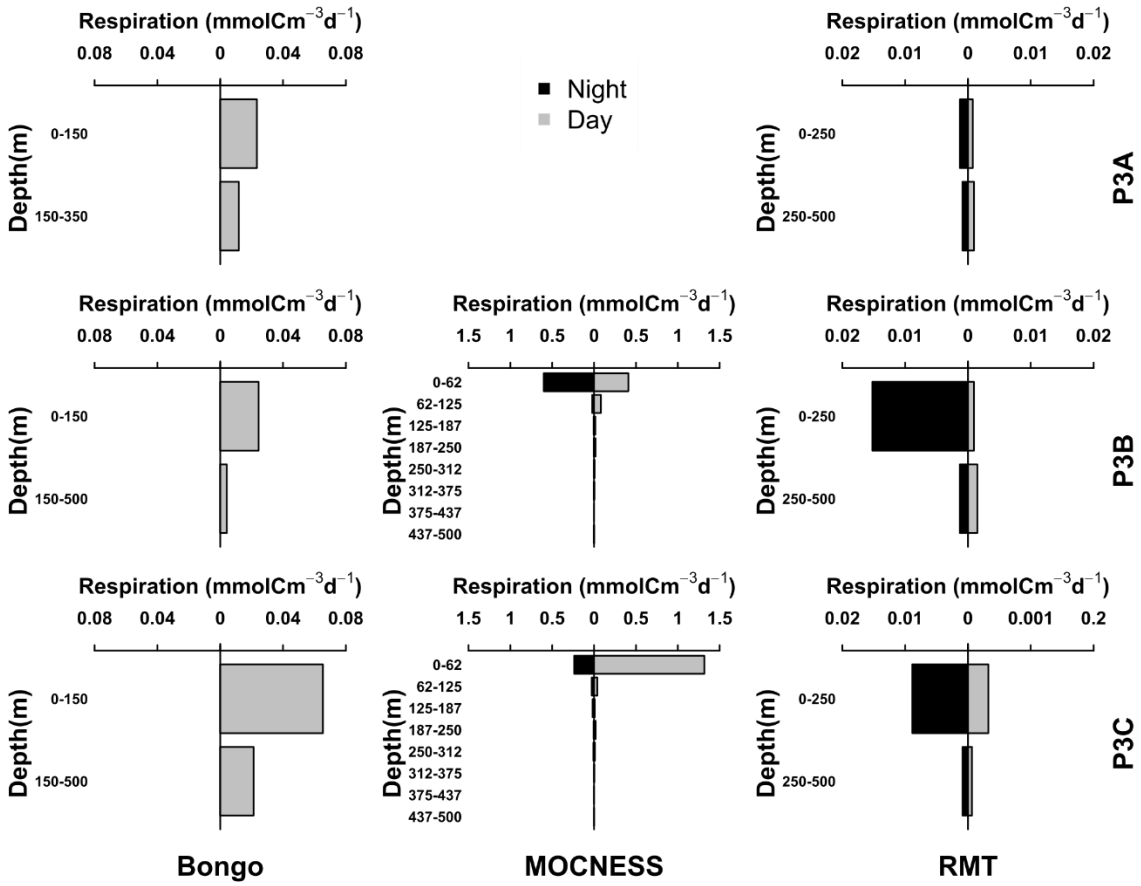
Respiration (mmolCm^{-3}d^{-1})
0.08 0.04 0 0.04 0.08
Night
Day
Depth(m)
0-150
150-350
0.02 0.01 0 0.01 0.02
0-250
250-500
P3A
0.08 0.04 0 0.04 0.08
0-150
150-500
1.5 1 0.5 0 0.5 1 1.5
0-62
62-125
125-187
187-250
250-312
312-375
375-437
437-500
0.02 0.01 0 0.01 0.02
P3B
0.08 0.04 0 0.04 0.08
0-150
150-500
1.5 1 0.5 0 0.5 1 1.5
0-62
62-125
125-187
187-250
250-312
312-375
375-437
437-500
0.02 0.01 0 0.001 0.2
P3C
Bongo
MOCNESS
RMT

Figure 4

1157

1158

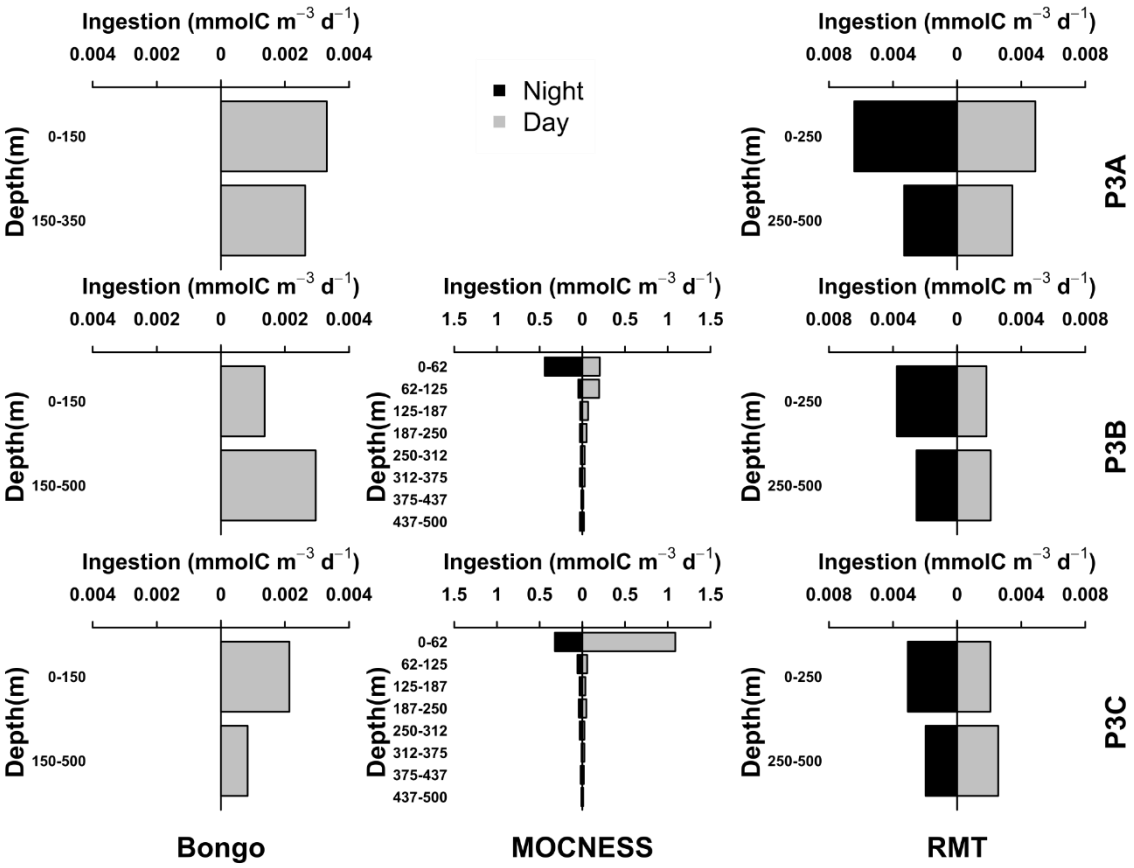

1159

1160 **Figure 5**

1161

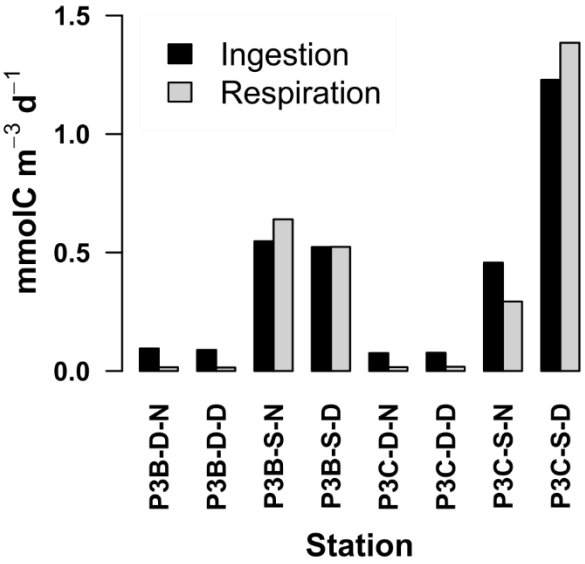

1162

1163 **Figure 6**

1164

Supplementary material

Table S1: Weighted mean carbon mass (mgC ind^{-1}) calculated using C mass per taxon (mgC, Ward et al., 2012) and abundance (N, ind m^{-3}). Equations are in the form:

$$\boldsymbol{Weighted\ C\ (mg\ ind^{-1})} = \frac{\boldsymbol{\Sigma\ C\ (mg)\ \times\ N\ (ind\ m^{-3})}}{\boldsymbol{\Sigma\ N\ (ind\ m^{-3})}}$$

	Weight mean C per individual (mg)	
Category	**5-150m**	**150-500m**
Cyclopoid copepods	0.0008	0.0009
Small calanoid copepods	0.01	0.01
Large calanoid copepods	0.22	0.23
Rhincalanus gigas	0.71	0.93
Metridia spp.	0.17	0.13
Polychaeta	0.66	0.66
Gastropoda	0.10	0.10
Ostracoda	0.009	0.009
Appendicularia	0.0002	0.0002
Euphausiacea	1.20	1.67

Table S2: Regression equations determined from ETS derived respiration and wet mass (WM, mg) measurements. *Euphausia superba* and *Thysanoessa* spp. equations are in the form:

Ln (Respiration (μlO_2 Ind^{-1} h^{-1}) = a_o + a_1 × ln (WM)

For fish, the equation is in the form:

Ln (Respiration (μlO_2 $mgWM^{-1}$ h^{-1}) = a_o + a_1 × ln (WM)

Species/group	**a_0**	**a_1**	**R^2**
Fish	3.366 (±0.557)***	-0.663 (± 0.066)***	69%
Euphausia superba	-2.619 (±2.425)*	1.154 (± 0.352)**	42%
Thysanoessa spp.	-3.646 (±0.542)***	1.258 (±0.133)**	69%

Signif. codes: 0 '***' 0.001 '**' 0.01 '*'

Table S3: Regression equations recalculated from Ikeda (2014) and Ikeda (2016) used to calculate respiration rate. Equations are in the form:

$$\text{Ln (Respiration } (\mu l O_2\ Ind^{-1}\ h^{-1}) = a_o + a_1 \times \ln(M) - a_2 \times 1000/T - a_3 \times \ln(z)$$

Where M=mass (mg), T=temperature (K), and z=depth (m). Mass is dry mass (DM) with the exception of cephalopods where mass is wet mass (WM)

Species/group	a_0	a_1	a_2	a_3	R^2
Cephalopoda^	28.336 (± 7.459)***	0.779 (± 0.067)***	-7.910 (± 2.104)***	-0.365 (±0.083)***	90%
Cnidaria	25.229 (± 4.218)***	0.877 (± 0.037)***	-7.445 (± 1.218)***	-0.006 (±0.041)	91%
Thallicaea	16.394 (±8.49) .	0.721 (±0.1556)***	-4.827 (±2.468) .	0.418 (±0.201) .	56%
Ctenophora	2.548 (±4.914)	0.685 (± 0.106)***	-0.883 (±1.419)	-0.021 (±0.082)	72%
Chaetognatha	19.517 (±4.162)***	0.663 (±0.064)****	-5.523 (±1.219)***	-0.160 (±0.051)**	79%
Decapoda	28.869 (±3.099)***	0.872 (±0.052)***	-8.084 (±0.919)***	-0.124 (±0.050)*	87%
Amphipoda	11.461 (±3.589)**	0.746 (±0.058)***	-3.021 (±1.052)**	-0.168 (±0.046)***	83%
Mollusca	12.627 (±3.396)***	0.895 (±0.056)***	-3.652 (±0.983)***	-0.008 (±0.057)	84%
Polychaeta	5.750 (±14.649)	0.771 (±0.200)**	-1.325 (±4.288)	-0.253 (±0.150)	75%
Euphausiacea	14.136 (±2.181)***	0.755 (±0.049)***	-3.754 (±0.633)***	-0.110 (±0.031)**	88%

^ mass in WM for cephalopods

Signif. codes: 0 '***' 0.001 '**' 0.01 '*' 0.05 '.'

Table S4: Wet mass (WM, mg) to dry mass (DM, mg) conversions used computed in this study. All equations are significant at p<0.001. Equations are of the form:

log (DM) = a + b × log (WM)

Species/group	**a**	**b**	**R^2**
Salpa thompsoni	-0.9673	0.8769	96%
Euphausia triacantha	-0.8147	1.0562	96%
Euphausia superba	-0.8221	1.0312	96%
Themisto gaudichaudii	-1.1188	1.1651	90%
Thysanoessa spp.	-0.9711	1.1698	97%

Individual specimens were defrosted on absorbent paper, transferred into pre-weighed glass vials and weighed to calculate WM. Where necessary, multiple individuals were weighed in one vial to give sufficient biomass for measurement. Samples were then lyophilised in a freeze-dryer for 48 hours, before being re-weighed to give DM. Regression equations were obtained based on multiple replicates per species.

Table S5: Wet mass (WM, mg) to dry mass (DM, mg) conversions from the literature used where we did not have our own measurements, and where DM was necessary for allometric respiration rate calculations. Equations are in the form:

$\log(DM) = a + b \times \log(WM)$

with the exception of Decapoda, which has the form:

$DM = a \times WM$

Species/group	**a**	**b**	**Reference**
Pteropoda	-0.55	0.8	Kiørboe (2013)
Amphipoda	-0.57	0.92	
Cnidaria	-1.33	0.99	
Ctenphora	-1.4	0.98	
Siphonphora (Cnidaria)	-1.33	0.99	
Euphausiacea	-0.69	1.03	
Polychaeta	-0.486	0.588	Mizdalski (1988)
Decapoda ^	0.179		Podeswa (2012)

^Note difference in form of equation

Table S6: Daily rations from this study (stations P3A-C) and the literature, used where we did not have our own measurements, applied to biomass measurements to calculate community ingestion.

Species/group	Daily ration (%)	Reference
Oithona similis C5-6 P3A 0-150m	35.4 ± 3.2	This study
Oithona similis C5-6 P3C 0-150m	24.8 ± 30.0	
Oithona similis C5-6 150-500m	19.9 ± 20.4	
Oithona similis C3-4 P3B	114.0 ± 29.6	
Oithona similis C3-4 P3C	62.1 ± 7.5	
Calanoides acutus C5 P3A	0.50 ± 0.37	
Calanoides acutus C5 P3B	0.96 ± 0.67	
Calanoides acutus C5 P3C	2.79 ± 0.83	
Rhincalanus gigas C6F P3A	2.91 ± 4.19	
Rhincalanus gigas C6F P3B	1.98 ± 1.70	
Rhincalanus gigas C6F P3C	1.64 ± 1.09	
Ctenocalanus spp. C5-6	9.76 ± 1.77	
Metridia spp. C6	8.65 ± 3.07	
Euphausia superba	3.1	Froneman et al. (1996)
E. crystallorophias	1.2	
Salpa thompsoni	72.7	
Vibilia antarctica	0.4	
Thysanoessa macrura adults	1.1	
T. macrura juveniles	2.3	
Myctophids (applied to all fish)	3.0	Pakhomov et al. (1996)
Amphipoda	0.5	Froneman et al. (2000)
Chaetognatha	5.0	Giesecke and González (2008)
Cephalopoda	1.7	Brodeur et al. (1999)

Figure S1: Day/night acoustic profiles during P3A

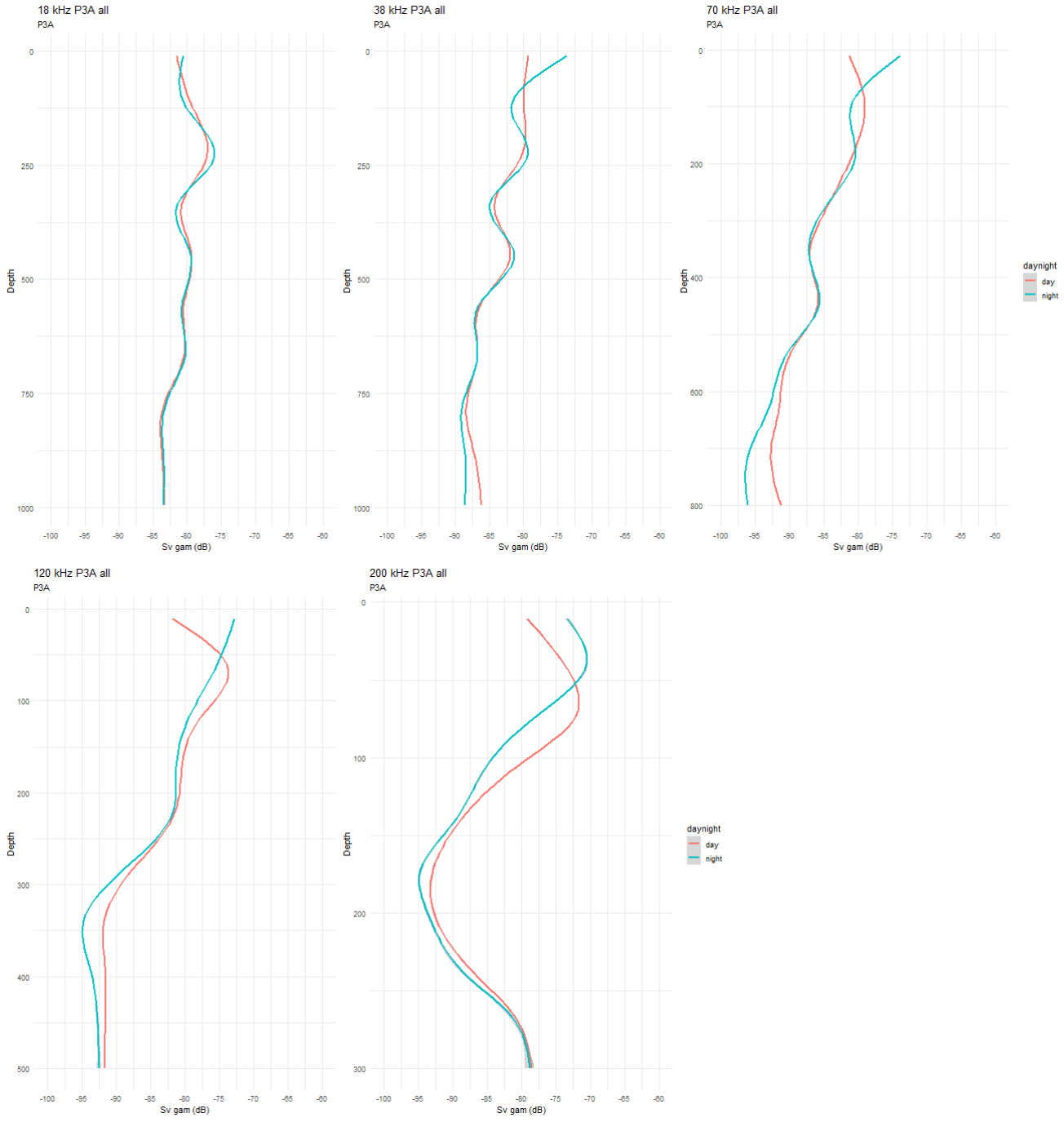

Figure S2: Day/night acoustic profiles during P3B

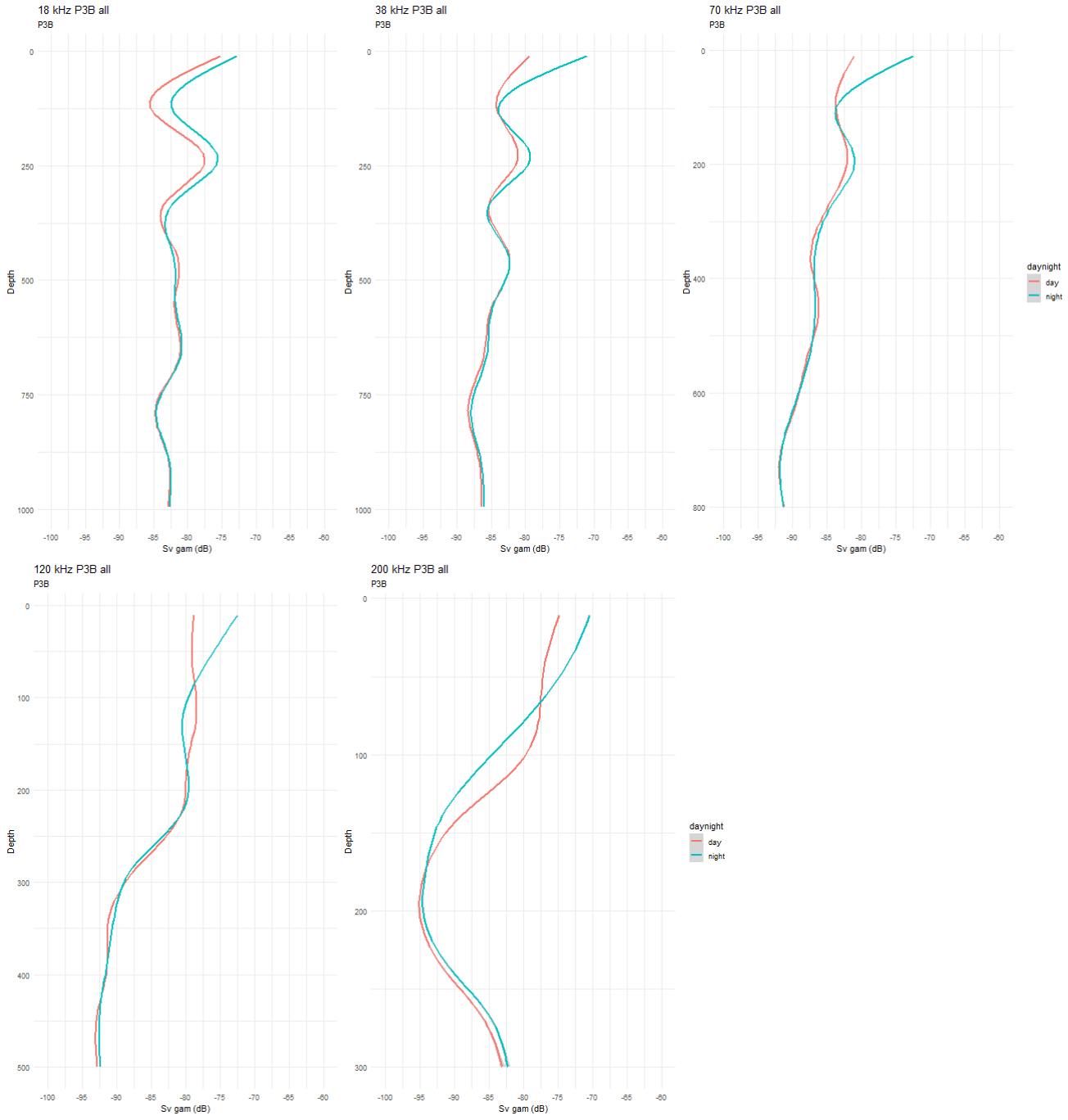

Figure S3: Depth profiles of mean (± s.e.) temperature (°C) and mean size of individual mesozooplankton (mmolC) binned according to MOCNESS depth strata, and carbon specific respiration (% d^{-1}) at in situ temperatures of mesozooplankton collected by the Bongo net (>100 μm) during station P3C and the Mammoth net (>300 μm) during stations P3A and P3C.

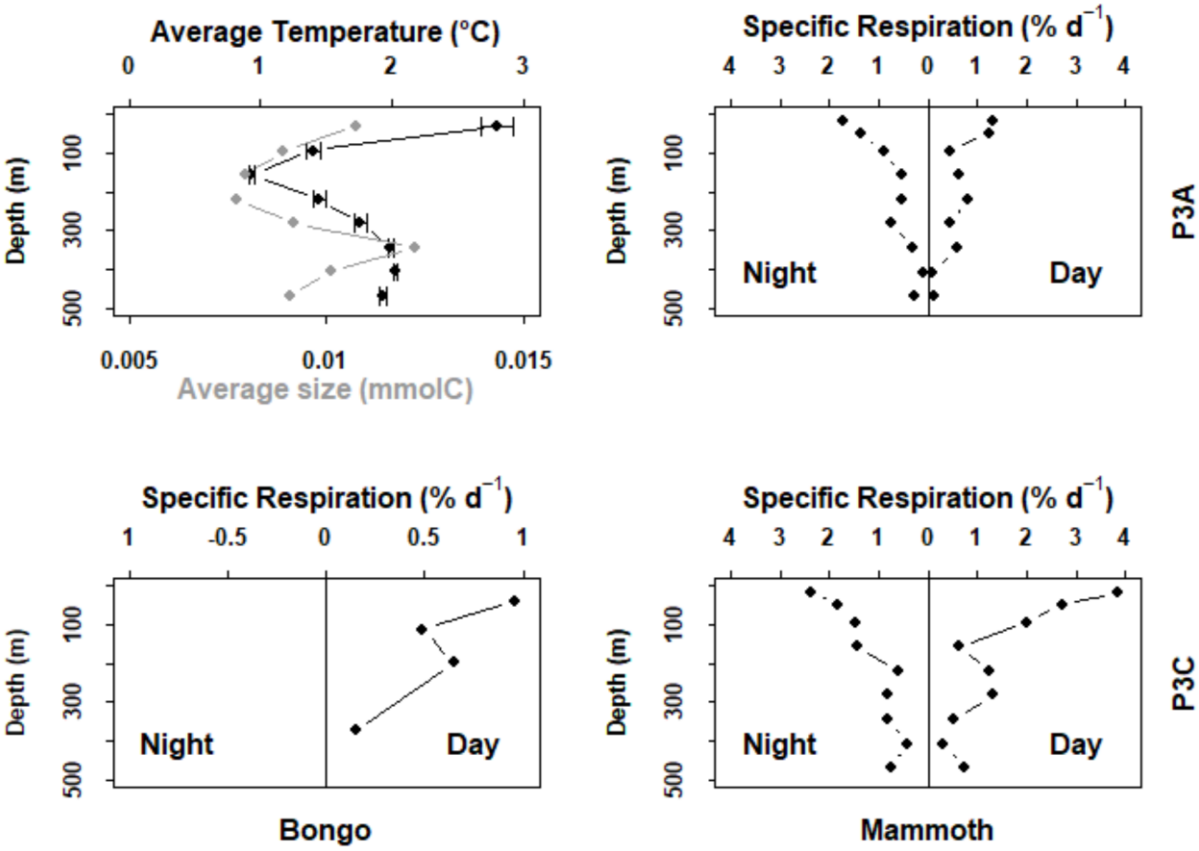

Figure S4: A) Composition (%) of incubation water (initial) and particles ingested (diet) by copepods during stations P3A, P3B and P3C: OS-S = *Oithona similis* stage C5-6 incubated in shallow water, OS-D = *O. similis* stage C5-6 incubated in deep water, OS = *O. similis* stage C5-6, OS-J = *O. similis* stage C3-4, CA = *Calanoides acutus* stage C5, RG = *Rhicalanus gigas* stage C6, CT = *Ctenocalanus* spp. stage C5-6, ME = *Metridia* spp. C6. See Table 1 for further details. B) Carbon specific ingestion (% d^{-1}) of copepods collected during station P3A, P3B and P3C. P3A-D = deep incubation water, P3A-S = shallow incubation water. All other measurements were made with shallow incubation water. Note the different scales on the y-axes. See Table 2 for further details.

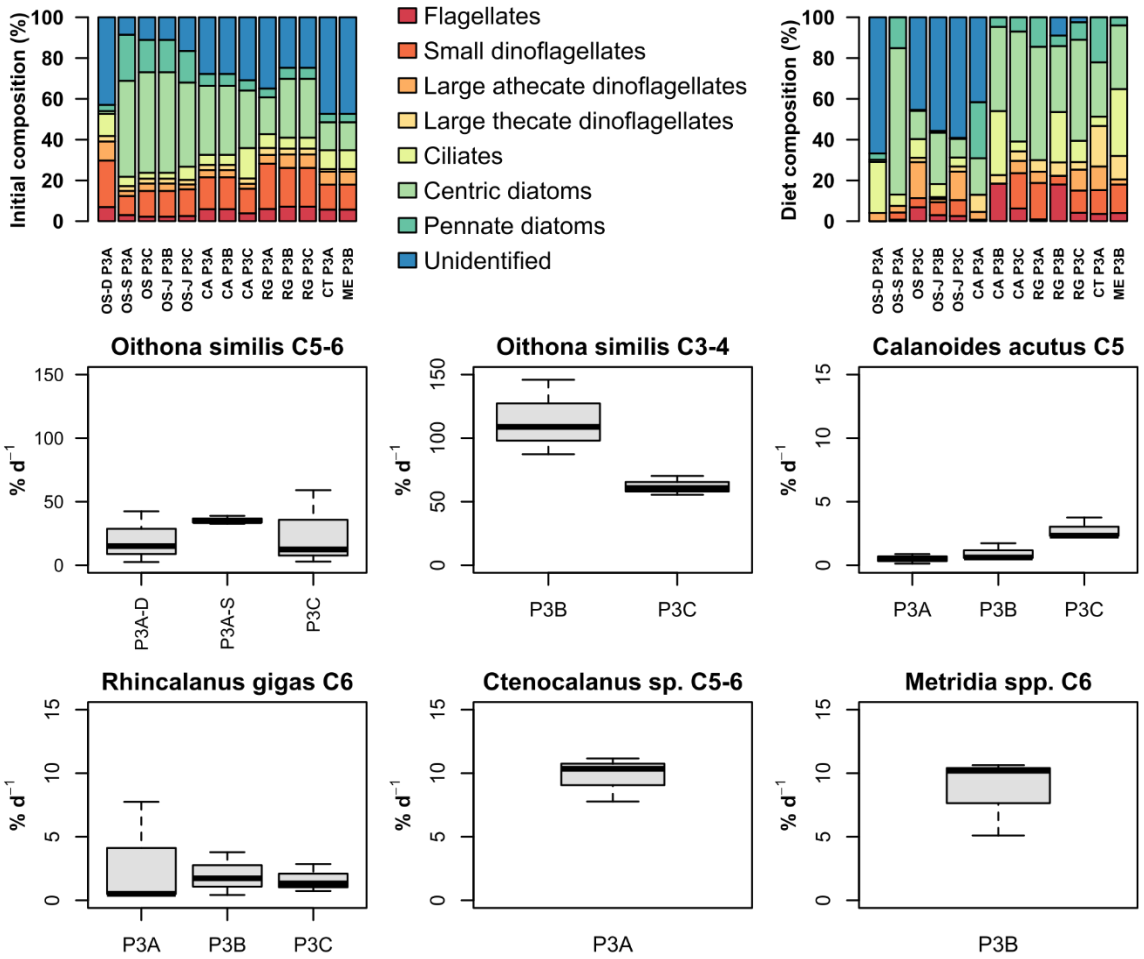

Figure S5: Seasonal distribution of *Calanoides acutus* interpolated from abundance data provided by Andrews (1966) for the Scotia Sea region of the Southern Ocean. Black dots represent depth and time of year of sampling points. Data covers a single 12-month period but is repeated to facilitate the interpolation procedure.

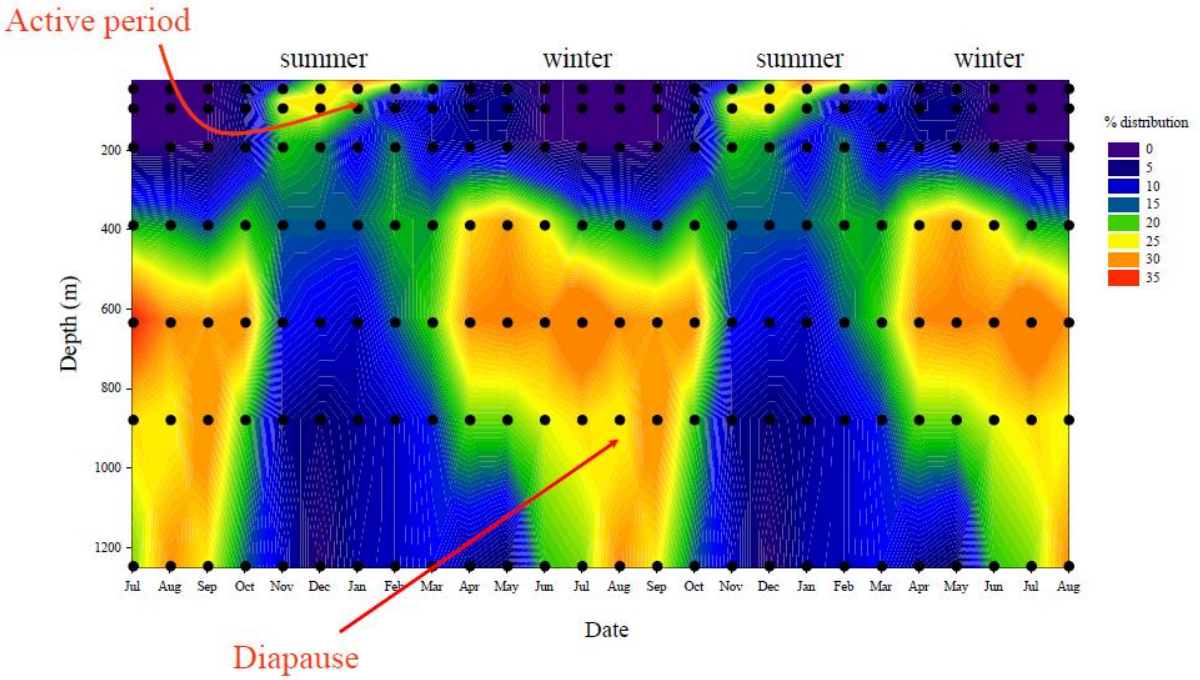

Data from Andrews (1966)